





Asteroid 2008 TC₃, not a polymict ureilitic but a polymict C1 chondrite parent body? Survey of 249 Almahata Sitta fragments

Addi BISCHOFF ^{*1}, Lukas BANNEMANN¹, Stephan DECKER², Samuel EBERT ¹,
Siegfried HABERER³, Ursula HEITMANN¹, Marian HORSTMANN⁴, Kerstin I. KLEMM¹,
Ann-Kathrin KRAEMER⁵, Sarah LENTFORT¹, Markus PATZEK ¹, Jakob STORZ ¹, and
Mona WEYRAUCH⁶

¹Institut für Planetologie, University of Münster, Wilhelm-Klemm-Str. 10, 48149 Münster, Germany

²Meteorite-Museum, Oberstrasse 10a, 55430 Oberwesel, Germany

³Haberer-Meteorite, Rene-Schickelestr. 28, 79117 Freiburg, Germany

⁴Beusselstraße 38, 10553 Berlin, Germany

⁵Institut für Geologische Wissenschaften, Freie Universität Berlin, Malteserstr. 74-100, 12249 Berlin, Germany

⁶Institut für Erdmessung, Leibniz Universität Hannover, Schneiderberg 50, 30167 Hannover, Germany

*Corresponding author. E-mail: bischoa@uni-muenster.de

(Received 03 February 2022; revision accepted 04 April 2022)

Abstract—On October 7, 2008, the asteroid 2008 TC₃ exploded as it entered the Earth's atmosphere, producing significant dust (in the atmosphere) and delivering thousands of stones in a strewn field in Sudan, collectively known as the Almahata Sitta (AhS) stones. About 600 fragments were officially recovered in 2008 and 2009. Further rocks were collected since the fall event by local people. From these stones, 249 were classified at the Institut für Planetologie in Münster (MS) known as MS-xxx or MS-MU-xxx AhS subsamples. Most of these rocks are ureilitic in origin (168; 67%): 87 coarse-grained ureilites, 60 fine-grained ureilites, 15 ureilites with variable texture/mineralogy, four trachyandesites, and two polymict breccias. We identified 81 non-ureilitic fragments, corresponding to 33% of the recovered samples studied in Münster. These included chondrites, namely 65 enstatite chondrites (43 EL; 22 EH), 11 ordinary chondrites (OC), one carbonaceous chondrite, and one unique R-like chondrite. Furthermore, three samples represent a unique type of enstatite achondrite. Since all AhS stones must be regarded as individual specimens independent from each other, the number of fresh ureilite and enstatite chondrite falls in our meteorite collections has been increased by several hundred percent. Overall, the samples weigh between <1 and 250 g and have a mean mass of ~15 g. If we consider—almost 15 years after the fall—the mass calculations, observations during and after the asteroid entered the atmosphere, the mineralogy of the C1 stones AhS 91A and AhS 671, and the experimental work on fitting the asteroid spectrum (e.g., Goodrich et al., 2019; Jenniskens et al., 2010; Shaddad et al., 2010), the main portion of the meteoroid was likely made of the fine-grained (carbonaceous) dust and was mostly lost in the atmosphere. In particular, the fact that C1 materials were found has important implications for interpreting asteroid 2008 TC₃'s early spectroscopic results. Goodrich et al. (2019) correctly suggested that if scientists had not recovered the “water-free” samples (e.g., ureilites, enstatites, and OC) from the AhS strewn field, 2008 TC₃ would have been assumed to be a carbonaceous chondrite meteoroid. Considering that the dominating mass of the exploding meteoroid consisted of carbonaceous materials, asteroid 2008 TC₃ cannot be classified as a polymict ureilite; consequently, we state that the asteroid was a polymict carbonaceous chondrite breccia, specifically a polymict C1 object that may have formed by late accretion at least 50–100 Ma after calcium–aluminum-rich inclusions.

INTRODUCTION

On October 6, 2008, a small asteroidal body was detected at 06:39 UTC by Richard Kowalski at the automated Catalina Sky Survey telescope at Mt. Lemmon Observatory (Arizona; Chesley et al., 2008; Kowalski, 2008; McGaha et al., 2008; Yeomans, 2008). Shortly after the discovery, its orbit was calculated; they predicted an impact on Earth about 19 h later (Jenniskens, Shaddad, and The Almahata Sitta Consortium, 2009; Jenniskens, Shaddad, Numan, et al., 2009; McGaha et al., 2008). The object was designated as asteroid 2008 TC₃.

Before entering the atmosphere, the reflectance spectrum of 2008 TC₃ was obtained in the 0.5–1 μm range (Hiroi, Jenniskens, Bishop & Shatir, 2010; Hiroi, Jenniskens, Bishop, Shatir, et al., 2010; Jenniskens, Shaddad, Numan, et al., 2009; Jenniskens et al., 2010). Scientists also found that it closely matched F-type asteroids in the Tholen taxonomy (Tholen & Barucci, 1989), whereby F-type asteroids are considered to belong to the C complex of dark (carbonaceous) asteroids (DeMeo et al., 2009, 2015; Tholen & Barucci, 1989), while ureilites were thought to derive from S-type asteroids (Gaffey et al., 1993). The complexity of asteroid surfaces with respect to their Tholen classification and how they can be related to known meteorite groups is not always straightforward. Tanbakouei et al. (2020) have shown for the case of comet 2P/Enke how the reflectance spectra are best represented by two anomalous ungrouped chondrites rather than established chondrite groups and hypothesized that these two meteorites could be rare surviving samples either from the Taurid complex or another compositionally similar body. Considering the asteroid 2008 TC₃ event, by consequence, Goodrich et al. (2019) correctly surmised that if no “water-free” samples (including all types of ureilitic lithologies and by far most chondrites) were recovered from the Almahata Sitta strewn field, 2008 TC₃ would have to be assumed to be a carbonaceous chondrite based on spectral data. Considering data from Shaddad et al. (2010) on the size of the asteroid and the density of meteorite finds, one can calculate that the overwhelming portion of the meteoroid (~99%) was made of fine-grained (carbonaceous) dust. Furthermore, almost all of this fine-grained material was lost in the atmosphere, as was observed via the huge dust clouds visible in images taken after asteroid 2008 TC₃ broke up in the atmosphere (Fig. 1). Shaddad et al. (2010) provide detailed information of the atmospheric breakup characteristics that will not be repeated in this study. Mass calculations of 2008 TC₃ obtained by linking laboratory measurements of the albedo of a ureilitic

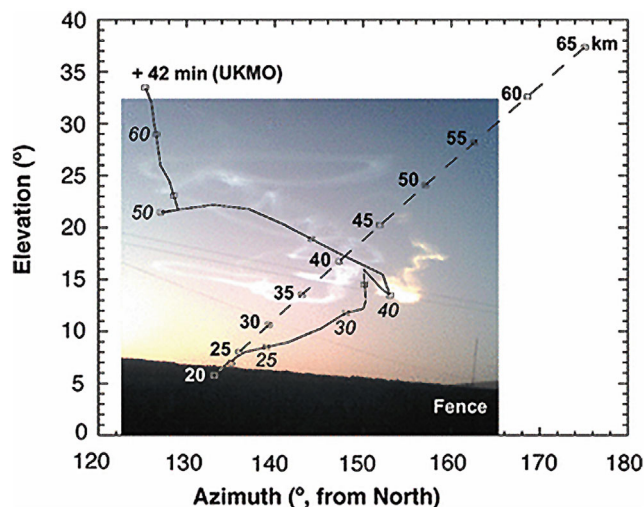


Fig. 1. As presented as fig. 3 in Shaddad et al. (2010), the dust train is shown as seen from Wadi Halfa +42 min after the fireball. The calculated trajectory of the asteroid and the dust trail as propagated by the UKMO wind model (Swinbank & O'Neill, 1994) are also presented. The part of the train penetrating deepest in the atmosphere is colored red, which is due to the rising sun as seen from 40 km altitude at that time. Figure reproduced with permission of Muawia Shaddad. (Color figure can be viewed at wileyonlinelibrary.com.)

fragment (0.046; Jenniskens, Shaddad, Numan, et al., 2009) and an assumed density yielded a mass of ~80 tons. Welten et al. (2010) and Kozubal et al. (2011) pointed out that a higher porosity (i.e., lower density) is more likely resulting in a mass of only ~40–50 tons, which would agree with satellite observations of the fireball (~35–65 tons; Borovicka & Charvat, 2009). However, the albedo of 0.046 for the measured ureilitic fragment might have been too low as stated by Hiroi, Jenniskens, Bishop, Shatir, et al. (2010), who suggest an average of 0.10–0.12. This, however, would result in a pre-entry mass of only ~20 tons that is in strong contrast to all the other measurements (Kohout et al., 2011). This contrast can be solved by having a high abundance of C1 dust in asteroid 2008 TC₃ with low albedo: An albedo of ~0.05 due to the high amount of C1 dust would result in a higher calculated mass similar to that calculated using the albedo measured by Jenniskens, Shaddad, Numan, et al. (2009) and again in agreement with mass estimates by other observations.

At the time of the first written report on classifying Almahata Sitta (AhS) samples (Horstmann & Bischoff, 2014), about 700 meteorite fragments were recovered from the strewn field, and 110 of these were studied in detail (about 25 by the consortium led by P. Jenniskens and about 80 at the Institut für Planetologie [University of Münster]). Shaddad et al. (2010) reported that in four expeditions from December 2008 to December 2009, 588 meteorites had been recovered, totaling

10.7 kg. This would give a mean mass of 18.2 g/sample. They also estimated the total mass of fallen rocks to be 39 ± 6 kg.

At first, AhS was classified as an anomalous polymict ureilite (Jenniskens, Shaddad, Numan, et al., 2009) mineralogically described by Zolensky et al. (2009) and Herrin et al. (2009). Soon afterward, 40 small pieces from different quite fresh fragments collected within the AhS strewn field were studied, revealing about 20 different lithologies (Bischoff, Horstmann, Laubenstein, et al., 2010; Bischoff, Horstmann, Pack, et al., 2010; Horstmann & Bischoff, 2010a, 2010b). Based on these findings, Bischoff, Horstmann, Laubenstein, et al. (2010) and Bischoff, Horstmann, Pack, et al. (2010) stated that AhS is not only a ureilitic meteorite but also a spectacular breccia containing clasts of both chondritic and achondritic lithologies. Here, we give details on a survey of 249 stones exclusively classified at the Institut für Planetologie in Münster.

As noted above, the overwhelming portion of the fine-grained material was probably lost in the atmosphere. The existence of C1-type materials among the AhS samples was proven much later, such as when Goodrich et al. (2019) discovered that stones recovered from asteroid 2008 TC₃ contained carbonaceous chondrite-dominated materials. Furthermore, samples AhS 91A and AhS 671—consisting of mixtures of carbonaceous and ureilitic materials—provide direct evidence that certain regions in asteroid 2008 TC₃ were similar in mineralogy to C1 chondrites. As indicated by Goodrich et al. (2019), this finding has important implications for asteroid spectroscopy, since such regions would have an ~ 2.7 μm absorption band due to the presence of their phyllosilicates.

Putting the spectroscopic observations and the findings of Goodrich et al. (2019) together with our investigations of a total of 249 different stones, we propose that asteroid 2008 TC₃ was a polymict carbonaceous chondrite breccia, specifically a polymict C1.

SAMPLES AND ANALYTICAL METHODS

All MS-MU samples (MS-MU-001–MS-MU-065) were collected in 2009. This is different from the MS samples: MS-D, MS-CH, and MS-7–MS-207 collected in 2009, whereas all samples starting from MS-208 onward were recovered in 2014, except for MS-321 and MS-323, which were also recovered in 2009. All samples are presented in Supplement S1 in the supporting information.

A total of 249 stones from the AhS strewn field were used to make thin and thick sections prepared at the Institut für Planetologie (Münster), which were

studied by optical and electron optical microscopy. A ZEISS polarizing microscope (Axiophot) was used for optical microscopy in transmitted and reflected light.

A JEOL 6610-LV scanning electron microscope (SEM) at the University of Münster was used to study the fine-grained textures and to identify the different mineral phases. Using the SEM for quantitative analysis, samples and appropriate mineral standards were measured at an excitation voltage of 20 kV, and the beam current was constantly controlled by a Faraday cup. The attached energy dispersive X-ray spectroscopy (EDS) system was used for chemical characterization and for analyses of the different mineral constituents. Standard (Astimex) olivine (Mg, Fe, Si), jadeite (Na), plagioclase (Al), sanidine (K), diopside (Ca), rutile (Ti), chromium-oxide (Cr), rhodonite (Mn), and pentlandite (Ni) were used as natural and synthetic standards. The EDS analyses used the INCA analytical program provided by Oxford Instruments.

Quantitative mineral analyses were also obtained by microprobe analyses using the JEOL JXA 8530F electron probe micro-analyzer (EPMA) at the Institut für Mineralogie in Münster, which was operated at 15 kV and a probe current of 15 nA. Natural and synthetic standards were used for wavelength-dispersive spectrometry. Jadeite (Na), kyanite (Al), sanidine (K), chromium oxide (Cr), San Carlos olivine (Mg), hypersthene (Si), diopside (Ca), rhodonite (Mn), rutile (Ti), fayalite (Fe), apatite (P), celestine (S), Co-metal (Co), and nickel oxide (Ni) were used as standards for mineral analyses.

RESULTS

Physical Properties

Although many samples were collected shortly after the fall, others were collected much later (in 2014) and, thus, were affected by terrestrial alteration processes in the desert. These effects are usually weak and restricted to metals near the fusion crust showing some terrestrial alteration, which is visible in the form of thin rinds of Fe-(hydr)oxides (max. W1–2; Wlotzka, 1993).

The samples studied in Münster have highly variable masses (<1–250 g; Supplement S1). The calculated mean mass of ~ 15 g is close to the mean masses for ureilitic and non-ureilitic samples (16.6 versus 12.4 g, respectively; Table 1; Fig. 2). However, some significant differences can be seen: The fine-grained ureilites have a distinctly lower mean mass (9.6 g) than the coarse-grained ureilitic stones (22.6 g). Also, the 11 ordinary chondrites (OCs) have a relatively low mean mass (5.3 g). Most of the 249 samples are between 2.5 and 10 g.

Table 1. Number of AhS samples classified and studied in Münster and their masses.

	No. of samples	Mass (g)	Mean (g)
Ureilitic rocks	168	2783.5	16.6
Coarse-grained	87	1968.2	22.6
Fine-grained	60	575.2	9.6
Variable mineralogy/texture	15	115.6	7.7
Ureilitic breccias	2	7.7	3.8
Trachyandesites	4	116.8	29.2
Non-ureilitic rocks	81	1006.9	12.4
Enstatite chondrites	65	686.9	10.6
Enstatite achondrites	3	197.0	65.7
Ordinary chondrites	11	58.7	5.3
Carbonaceous chondrite	1	58.6	58.6
Rumuruti-like chondrite	1	5.7	5.7
All samples	249	3790.4	15.2

Mineralogy

Since 2009, 249 samples have been studied in Münster. From these samples, about 80 were characterized by Horstmann and Bischoff (2014). Further samples were briefly mentioned in Bischoff et al. (2015, 2016, 2019) and Bischoff, Kraemer, et al. (2018). Most of these rocks are ureilitic in origin (168; 67%)—87 coarse-grained ureilites, 60 fine-grained ureilites, 15 ureilites with variable texture or mineralogy, four trachyandesites, and two polymict breccias. Among the chondrites, we identified 65 enstatite chondrites (43 EL; 22 EH), 11 OCs, one carbonaceous chondrite, and one unique R-like chondrite. Furthermore, three samples were found to represent a unique type of enstatite achondrite (Harries & Bischoff, 2020). Thus, the 81 non-ureilitic fragments correspond to 33% of the recovered samples studied in Münster. The mineralogy and texture of the main groups of AhS stones have been characterized in detail by Horstmann and Bischoff (2014) and will not be repeated here. Instead, we give only brief descriptions and show typical samples via appropriate images; however, we do describe some newly observed extraordinary samples in more detail below.

Ureilitic Samples

Coarse-Grained Ureilites

Coarse-grained ureilites among the AhS samples have been mineralogically examined by several authors (e.g., Bischoff, Horstmann, Laubenstein, et al. 2010; Bischoff, Horstmann, Pack, et al. 2010; Bischoff et al., 2015, 2016, 2019; Bischoff, Kraemer, et al., 2018; Goodrich et al., 2014, 2016, 2018, 2019; Herrin et al.,

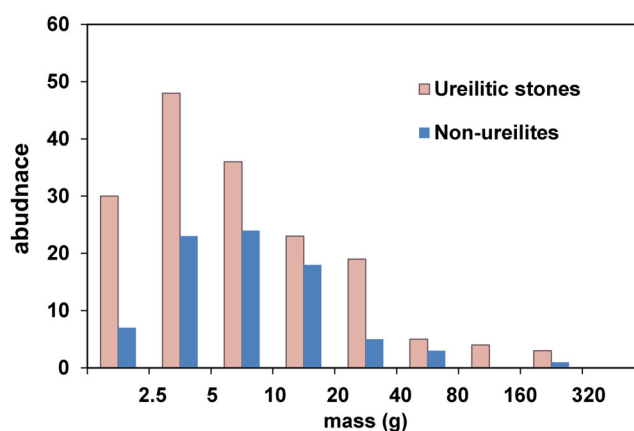


Fig. 2. Mass distribution of 249 Almahata Sitta stones studied in Münster. The most abundant ureilitic samples are in the mass range of 2.5–5 g, whereas the most abundant non-ureilites are between 5 and 10 g. (Color figure can be viewed at wileyonlinelibrary.com.)

2009, 2010; Horstmann & Bischoff, 2014; Horstmann, Bischoff, et al., 2012; Hutchins & Agee, 2012; Moehlmann, 2020, Storz et al., 2021; Zolensky et al., 2009; Zolensky, Herrin, Mikouchi, Ohsumi, et al., 2010; Zolensky, Herrin, Mikouchi, Satake, et al., 2010). Among the 249 samples in Münster, 87 can be classified as coarse-grained ureilites. They typically have grain sizes above 100 μm , with some rocks having sizes up to several millimeters, and they show variable modal abundances of olivine, low-Ca pyroxene, and augite. MS-MU-012 also contains plagioclase (Bischoff et al., 2015; Goodrich et al., 2016). Most coarse-grained ureilites were found to be olivine rich (please note that the apparent modal proportions may not be entirely representative of the host lithology because of the small size of the sample in many cases), but some are pyroxene rich (e.g., MS-16, MS-169, MS-MU-004, MS-298 [Fig. 3f], MS-303, MS-318). The coarse-grained ureilites MS-323 and MS-MU-034 weigh ~250 and ~222 g, respectively, and are the largest samples among the 249 stones studied. Typically, olivine-rich coarse-grained ureilites (Fig. 3) have larger grain sizes than pyroxene-rich samples, which tend to have grain sizes significantly below 1 mm. Similar to other ureilites studied prior to the asteroid 2008 TC₃ event, the AhS coarse-grained ureilites are characterized by reduction rims around olivine (and less obvious pyroxene) sprinkled with numerous tiny Fe metal grains. Considering the chemical compositions of olivine and pyroxenes, the coarse-grained AhS ureilites cover the full compositional spectrum previously known from ureilites (e.g., Goodrich et al., 2004; Mittlefehldt et al., 1998) and range from Mg-rich silicate core compositions (e.g., MS-288: Fa₄/Fs₄) to much Fe-richer

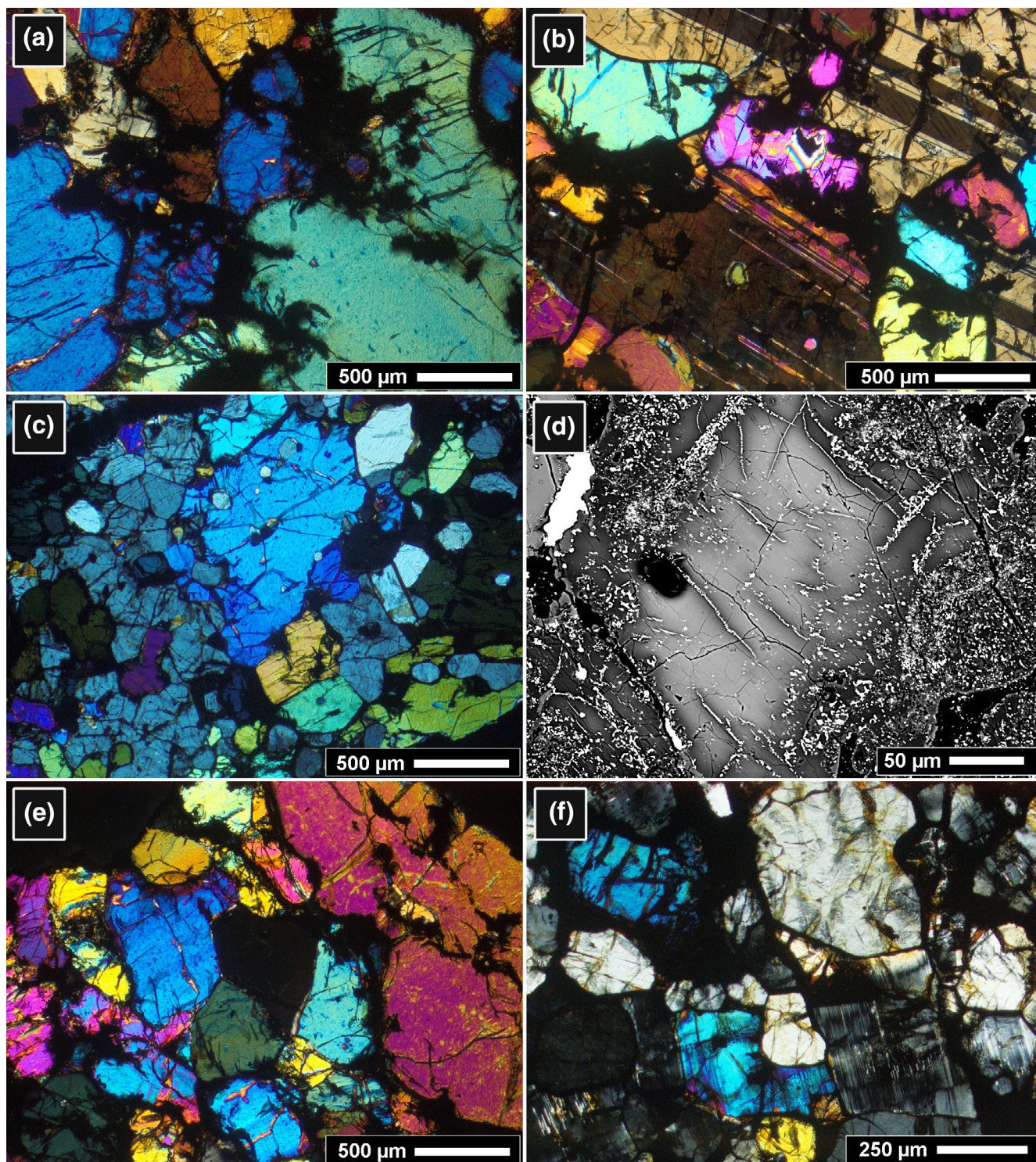


Fig. 3. Typical coarse-grained ureilites. a) MS-275 has millimeter-sized olivine grains. b) MS-MU-063 partly shows a poikiloblastic texture. c) MS-279 is coarse-grained but is more variable in grain size. d) The coarse-grained ureilite MS-MU-020 has strong reduction features in and around olivine. e) MS-260 has abundant olivine. f) Coarse-grained ureilite MS-298 is pyroxene rich. Images in polarized light with crossed nicols, except for (d) which is a backscattered electron (BSE) image. (Color figure can be viewed at wileyonlinelibrary.com.)

silicate core compositions (e.g., MS-310: Fa_{25}/Fs_{21} ; Fig. 4).

Fine-Grained Ureilites

Among the samples studied in Münster, 60 fine-grained ureilites were classified. Rocks of this type from the AhS collection (Figs. 5a–d) have also been studied by, for example, Jenniskens, Shaddad, Numan, et al. (2009); Bischoff, Horstmann, Laubenstein, et al. (2010); Bischoff, Horstmann, Pack, et al. (2010); Zolensky et al. (2009); Zolensky, Herrin, Mikouchi, Ohsumi, et al. (2010); Zolensky, Herrin, Mikouchi, Satake, et al. (2010); Herrin et al. (2009, 2010); Mikouchi, Zolensky, Ohnishi, et al. (2010); Mikouchi, Zolensky, Takeda, et al. (2010); Warren and Rubin (2010); Horstmann and Bischoff (2010a, 2014); Ross, Herrin, et al. (2011); Hutchins and Agee (2012); Horstmann (2013); Horstmann et al. (2013); Horstmann, Humayun, Fischer-Gödde, et al. (2014); Goodrich et al. (2014, 2018); Moehlmann (2020); and Storz et al. (2021). This type of rock shows strongly recrystallized (polycrystalline) and typically strongly reduced mineral assemblages, especially for olivine and to a lesser degree for pyroxene. Some of the fine-grained, often porous rocks are dominated by pyroxene (Zolensky, Herrin, Mikouchi, Satake, et al., 2010), while others are rich in olivine (Bischoff, Horstmann, Pack, et al., 2010; Warren & Rubin, 2010). The former coarse-grained silicates (especially olivines) are mosaiced, consisting of very small (10–50 μm) subgrains of olivine and pyroxene (Fig. 5); this texture is a result of strong shock and subsequent annealing. Due to the shock event, these fine-grained ureilites generally have a higher abundance of diamond shock-transformed from graphite (Bischoff et al., 1999) than coarse-grained ureilites. Chemically, as stated previously by Horstmann and Bischoff (2014), the main phases in fine-grained ureilites comprise a range of silicate compositions, which are generally similar to those in coarse-grained ureilites (Fig. 6). However, the reduction process more significantly affects olivine than low-Ca pyroxene (Fig. 6). One ultra-fine-grained rock (MS-185 with <10 μm grain size) was found with strongly reduced olivine, giving a maximum Fa content of 1.5 mol% (Horstmann & Bischoff, 2014; Horstmann, Bischoff, et al., 2012). Some fine-grained ureilites contain abundant and large metal and sulfide grains (Figs. 5d and 7).

Ureilite with Variable Grain Size and/or Untypical Mineralogy or Texture

Considering the review work of Horstmann and Bischoff (2014), this chapter will summarize their sections “Dark ureilites and ureilites with variable grain size” and “Ureilitic sulfide-metal assemblages.” All these

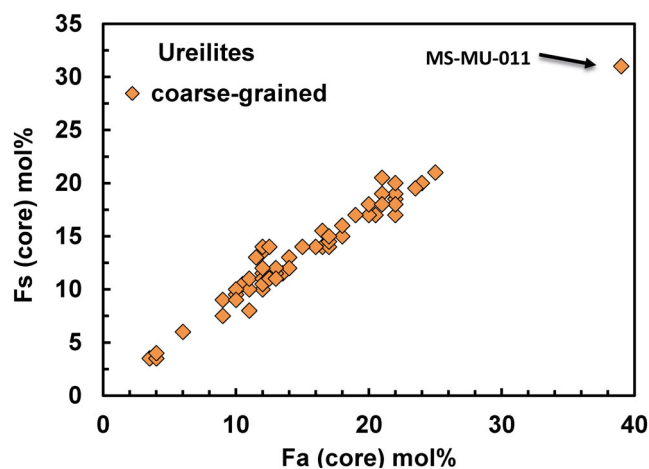


Fig. 4. Core compositions of olivine and low-Ca pyroxene in the investigated coarse-grained ureilites of the Almahata Sitta strewn field. The largest and most Fe-rich olivine (Fa_{39}) was found as a centimeter-sized fragment within the trachyandesite MS-MU-011 (see below). (Color figure can be viewed at wileyonlinelibrary.com.)

samples contain areas with a fine-grained or medium-size-grained texture, but some also contain mafic crystals with larger grain sizes (Fig. 8a) or parts having unusual sulfide–metal assemblages (MS-158, MS-166; Fig. 7), which have been described and analyzed in several AhS samples (Bischoff, Horstmann, Laubenstein, et al., 2010; Bischoff, Horstmann, Pack, et al., 2010; Horstmann, 2013; Horstmann et al., 2011a, 2013; Horstmann, Humayun, et al., 2012; Ross, Herrin, et al., 2011; Ross, Hezel, et al., 2011). As mentioned by Horstmann and Bischoff (2014), some ureilites (e.g., MS-25 and MS-190) appear dark in transmitted light due to numerous tiny inclusions of mainly Fe metal and minor FeS (Horstmann, Bischoff, et al., 2012). In other cases, some pyroxene and olivine grains of variable sizes appear as relics in the reduced fine-grained ground mass, often less affected by heavy reduction (Fig. 9a). In the cases of MS-254 and MS-MU-021, some large Fe-rich olivines exist (Fa_{22} and Fa_{26} , respectively), but we found no low-Ca pyroxenes with Fs contents above 10 mol% (Fig. 6). We cannot completely exclude the possibility that some of these samples are breccias due to reprocessing upon impact fragmentation and lithification.

Ureilitic Trachyandesites

Among the investigated AhS samples, four feldspar-rich fragments (MS-MU-011, MS-MU-035, MS-MU-065, and MS-277) were identified (Fig. 9). First results on the mineralogy, mineral chemistry, and oxygen isotope composition of MS-MU-011 (named ALM-A) were presented in Bischoff et al. (2013), where the rock was described as a basalt, based on its texture.

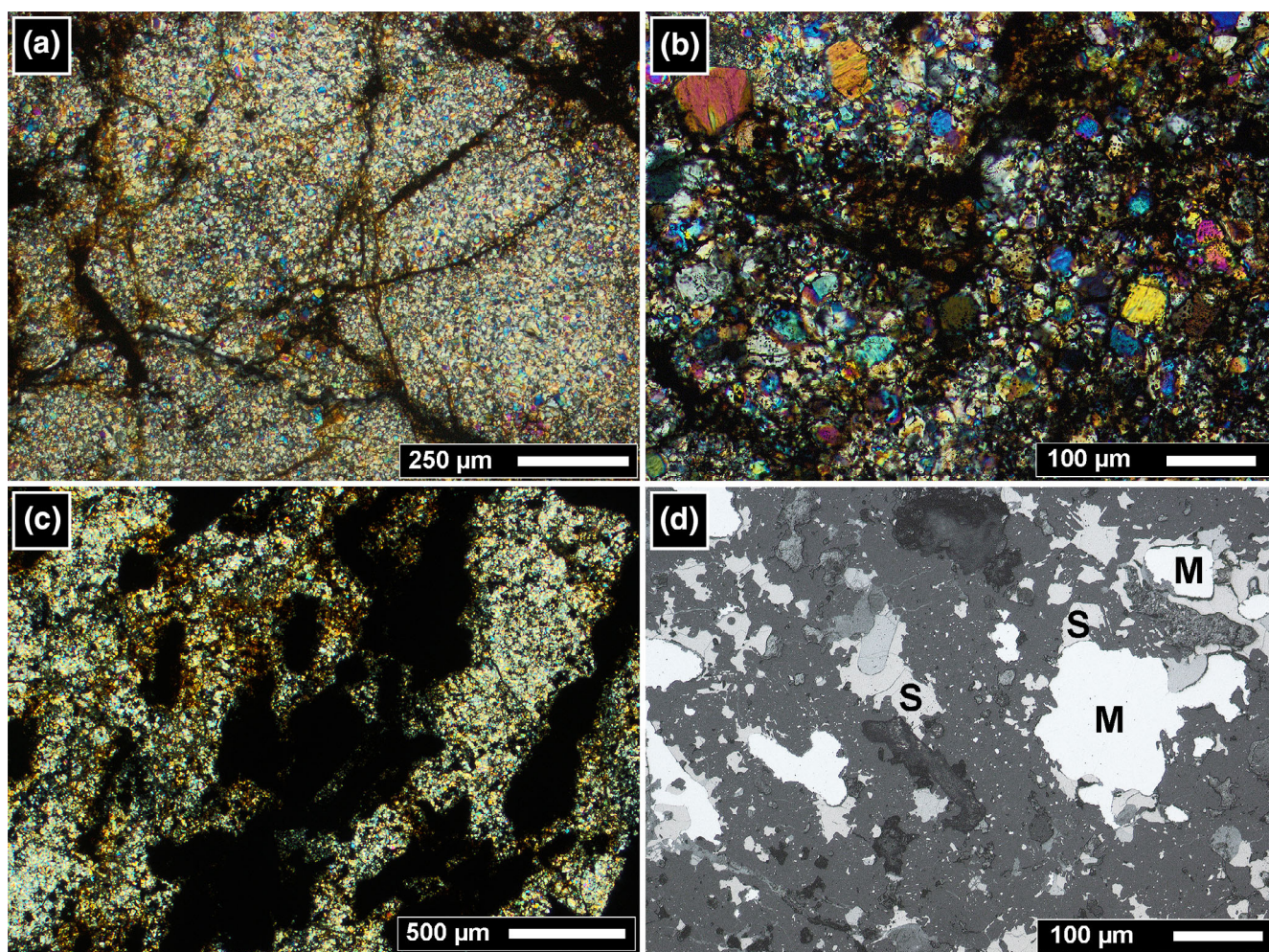


Fig. 5. Fine-grained ureilites. a) MS-299 is a typical fine-grained ureilite with subgrains of mosaic olivine in the 1–20 μm size range. b) MS-265 is a fine-grained ureilite with olivine subgrains up to $\sim 70 \mu\text{m}$. c) MS-MU-027 is a graphite-rich, fine-grained ureilite; the black areas are mainly made of C allotropes/polymorphs including graphite and diamond. d) The fine-grained ureilite MS-270 is shown with metal- (M, white) and sulfide-rich (S, yellow-brownish) areas. (Color figure can be viewed at wileyonlinelibrary.com.)

However, the bulk chemistry revealed that it is a trachyandesite (Bischoff et al., 2014). ALM-A was also studied by Amelin et al. (2015), Ward et al. (2017), Bast et al. (2017), Barnes et al. (2019), Collinet and Grove (2020a, 2020b), and Peterson et al. (2022). The rock mainly consists of abundant feldspar (anorthoclase and plagioclase [together $\sim 70 \text{ vol}\%$]) with subhedral, zoned plagioclase laths ($\sim \text{An}_{10-55}$) embedding Cr-bearing Ca pyroxene ($\sim \text{Fs}_{20-21}\text{Wo}_{36-37}$, Cr_2O_3 : $\sim 1 \text{ wt}\%$), and Ca-poor pyroxene ($\sim \text{Fs}_{35-37}\text{Wo}_{7-10}$; Bischoff et al., 2014; Horstmann & Bischoff, 2014). After MS-MU-011 was identified, very similar rocks were then found; MS-MU-035, MS-277, and MS-MU-065 (Fig. 9) have masses of 26.9, 11.03, and 54.7 g, respectively.

Upon further work on MS-MU-011, the sample was found to contain a cm-sized olivine-rich fragment within the trachyandesite. The olivine (Fa_{39}) embeds zoned

plagioclase (cores: $\sim \text{An}_{53}$) and low-Ca pyroxene (Fs_{31}) (Fig. 9b). This fragment may represent parts of the host rock (perhaps from the walls of the melt chamber) that may have contaminated the trachyandesitic melt.

Ureilitic Breccias

Within two AhS stones classified in Münster, fine-grained components were found. MS-266 is a polymict breccia that contains (mainly) ureilitic lithologies and a C1-clast (Bannemann, 2021). The ureilitic lithologies are dominated either by fine- (5–60 μm) or coarse-grained (>60 μm) olivine (Fo_{77-88} ; up to Fo_{99} in the reduced parts at their edges) and low-Ca pyroxene. The polymict rock also contains isolated masses of graphite (up to $\sim 300 \mu\text{m}$ in size) and grains of plagioclase ($\text{An}_{28.2}$ and $\text{An}_{4.7}$) as well as small metal (kamacite) and sulfide (troilite) grains or trails. Metal and sulfide are also

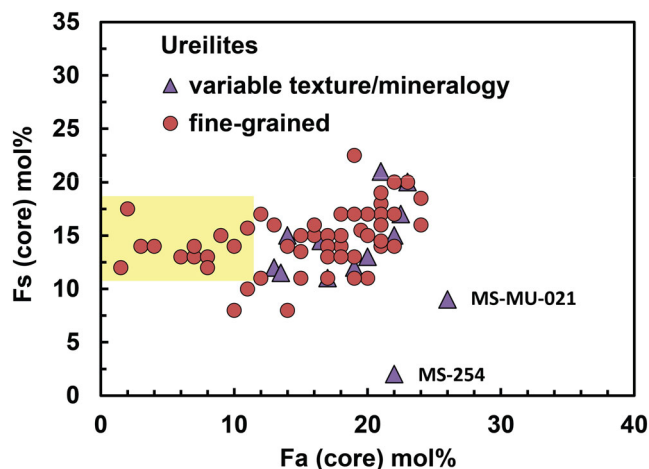


Fig. 6. Core compositions of olivine and low-Ca pyroxene in fine-grained ureilites (FG-Ure) and in ureilites with variable grain size and/or untypical mineralogy (variable texture/mineralogy) of the Almahata Sitta strewn field. In several cases, the reduction process more strongly affected the olivine; thus, samples with olivine cores of low Fa contents (\sim Fa₁₋₁₀) coexist with relatively FeO-rich low-Ca pyroxenes of Fs₁₂₋₁₈. In two cases (MS-254 and MS-MU-021), the opposite is observed. Within these samples, a small number of large Fa-rich olivines are embedded in fine-grained ureilitic lithologies (cf. Fig. 8a). (Color figure can be viewed at wileyonlinelibrary.com.)

found as an interstitial filling in fine-grained olivine-rich areas. The C1 lithology (Fig. 10a) is enclosed by ureilitic lithologies and consists of an extremely fine-grained matrix-like mixture predominantly of phyllosilicates, pyrrhotite grains, and clusters of magnetites typically found in C1 chondrites (e.g., Alfing et al., 2019; Bischoff et al., 2021; Fredriksson & Kerridge, 1988; Morlok et al., 2006) or as C1 clasts in other brecciated chondritic and achondritic rocks (e.g., Endreß et al., 1994; Funk et al., 2011; Goodrich et al., 2019; Patzek et al., 2018, 2019, 2020, 2021; Visser et al., 2018, 2019). A few components in the polymict breccia are neither ureilitic nor of a C1 type. These components include grains of olivine (e.g., Fo_{74.4}), (probably chondritic), orthopyroxene with Wo_{<1.0}, and merrillite. The ureilitic lithologies in MS-266 have similar textural, mineralogical, and compositional characteristics as other monolithic stones among the AhS rocks (see above). The C1 lithology in MS-266 is certainly different from CII materials and resembles C1 lithologies that have been found and characterized in some other AhS fragments (Goodrich et al., 2019).

Within the fine-grained ureilite breccia MS-296, unique clasts (or areas) occur that contain abundant metal-sulfide-rich spherules embedded in a fine-grained (probably) phyllosilicate-rich groundmass (Fig. 10b). These areas are typically close to metals and terrestrial

alteration products, and we cannot rule out the possibility that these areas were also modified by secondary processes in the desert.

Enstatite-Rich Samples—Enstatite Achondrites

Three of the investigated rocks from the AhS strewn field can be best classified as unique primitive achondrites (MS-MU-019, MS-MU-036, MS-245; Bischoff et al., 2015, 2016). MS-MU-036 is, at 177 g, one of the largest samples studied in Münster. Besides consisting of abundant pyroxene, all three have abundant metal (Fig. 11). The two unique achondritic lithologies of MS-MU-019 and MS-MU-036 contain three coexisting pyroxene species: orthoenstatite, clinoenstatite, and augite (Harries & Bischoff, 2020). We suggest that the silicate assemblage may resemble restites after extraction of melts of broadly basaltic and metal-sulfide composition from an enstatite chondrite protolith.

Enstatite-Rich Samples—Enstatite Chondrites

Among the AhS stones, 65 enstatite (E) chondrites were studied in Münster representing distinct E chondrite parent lithologies (Fig. 12). Both EL and EH chondrites were identified as well as all different subtypes (EH_a, EH_b, EL_a, EL_b; Figs. 13 and 14) as defined by Weyrauch et al. (2018). The petrologic types range from primitive type 3 (e.g., the EH_a3-chondrites MS-14 and MS-244) to highly metamorphosed rocks (e.g., EH_a6-chondrite MS-313 and EL_b6-chondrite MS-MU-050). MS-MU-055 is classified as an EL_b impact melt rock breccia, and MS-179 is an EL breccia with obvious fragments of different petrologic (types 3–5; Fig. 12a).

Many AhS E chondrite samples have been described in the past (e.g., Bischoff, Horstmann, Laubenstein, et al., 2010; Bischoff, Horstmann, Pack, et al., 2010; El Goresy et al., 2011, 2012, 2017; Hilker, 2017; Horstmann, 2010, 2013; Horstmann & Bischoff, 2014; Horstmann et al., 2011b, 2013; Horstmann, Bischoff, et al., 2012; Horstmann, Humayun, & Bischoff, 2014; Kimura et al., 2021; Lin et al., 2011; Moehlmann, 2020; Riebe et al., 2014, 2017; Storz et al., 2021; Weyrauch et al., 2014, 2018).

Horstmann and Bischoff (2014) mentioned that several samples (e.g., MS-14, MS-155, and MS-164) were found with clear indications for a partial melt origin. This is especially the case for some primitive type 3 E chondrites. Horstmann, Humayun, and Bischoff (2014) favored a pre-accretionary melt origin of the metal-silicate assemblages found in many AhS primitive E chondrites. Based on mineral chemical

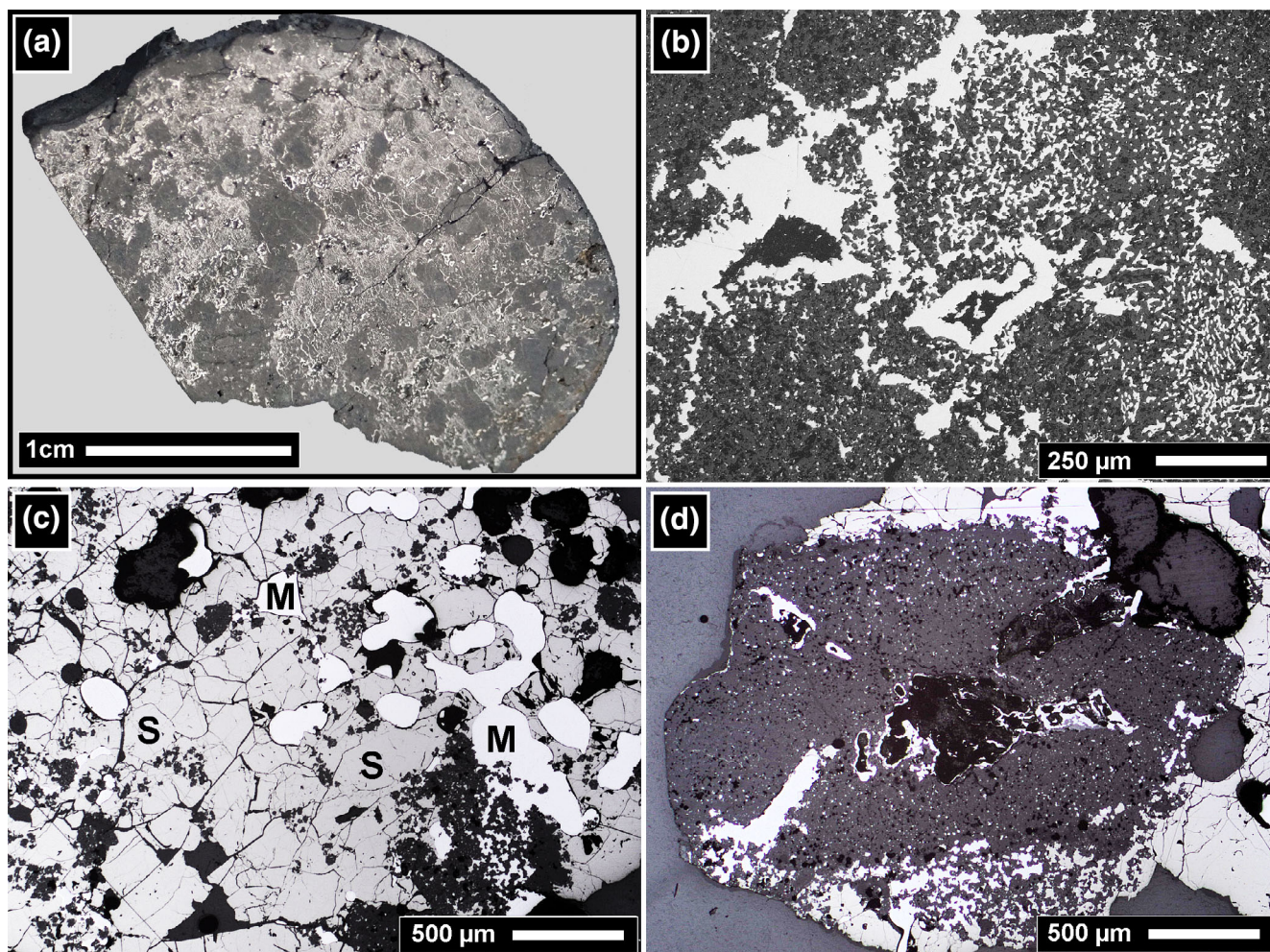


Fig. 7. a) Fine-grained ureilite MS-319, where the cut surface of the stone shows abundant small metal and sulfide grains (~3 cm in longest direction). b) A small metal-rich area of MS-319 shown in detail (reflected light). c) The metal–sulfide-rich area of MS-158, a ureilite with untypical mineralogy. d) Silicate-rich area in MS-158 surrounded by abundant sulfide and some metal grains. c, d) BSE images. (Color figure can be viewed at wileyonlinelibrary.com.)

constraints, these authors ruled out in situ impact melt origin of these metal–silicate assemblages also found in many other primitive E chondrites. Kimura et al. (2021), who studied the EL₃ chondrite MS-177, also considered a complex formation history and that distinct features may be related to processes before accretion to the parent body.

Ordinary Chondrites

From the AhS samples studied in Münster, 11 were identified as OC (Fig. 15), which some authors originally considered to be unrelated to AhS (e.g., Rumble et al., 2010). Among these OC are nine H, one L, and one LL chondrite(s). Most of the OC are metamorphosed and show equilibrated olivine and pyroxene compositions (Fig. 16). Only within two H4

chondrites (MS-MU-043, –048) do the compositions of low-Ca pyroxene still show minor variation. In contrast, the most spectacular OC MS-MU-060 is highly unequilibrated (L3) and shows a well-preserved chondritic texture (Figs. 15a and 15b). The compositions of olivine and pyroxene are highly variable, with Fa₁₋₄₆ (mean: 14.5 ± 9.9 mol%) and Fs₁₋₂₂ (mean: 10.5 ± 7.6 mol%), respectively. The L chondrite classification is based on the abundance of metal (~4 vol%). Data on AhS OC rocks were earlier reported by, for example, Bischoff, Horstmann, Laubenstein, et al. (2010); Bischoff, Horstmann, Pack, et al. (2010); Bischoff et al. (2015); Bischoff, Kraemer, et al. (2018); Zolensky, Herrin, Mikouchi, Ohsumi, et al. (2010); Warren and Rubin (2010); Meier et al. (2010); Horstmann, Bischoff, et al. (2012); Horstmann and Bischoff (2014); and Riebe et al. (2014, 2017). Some of

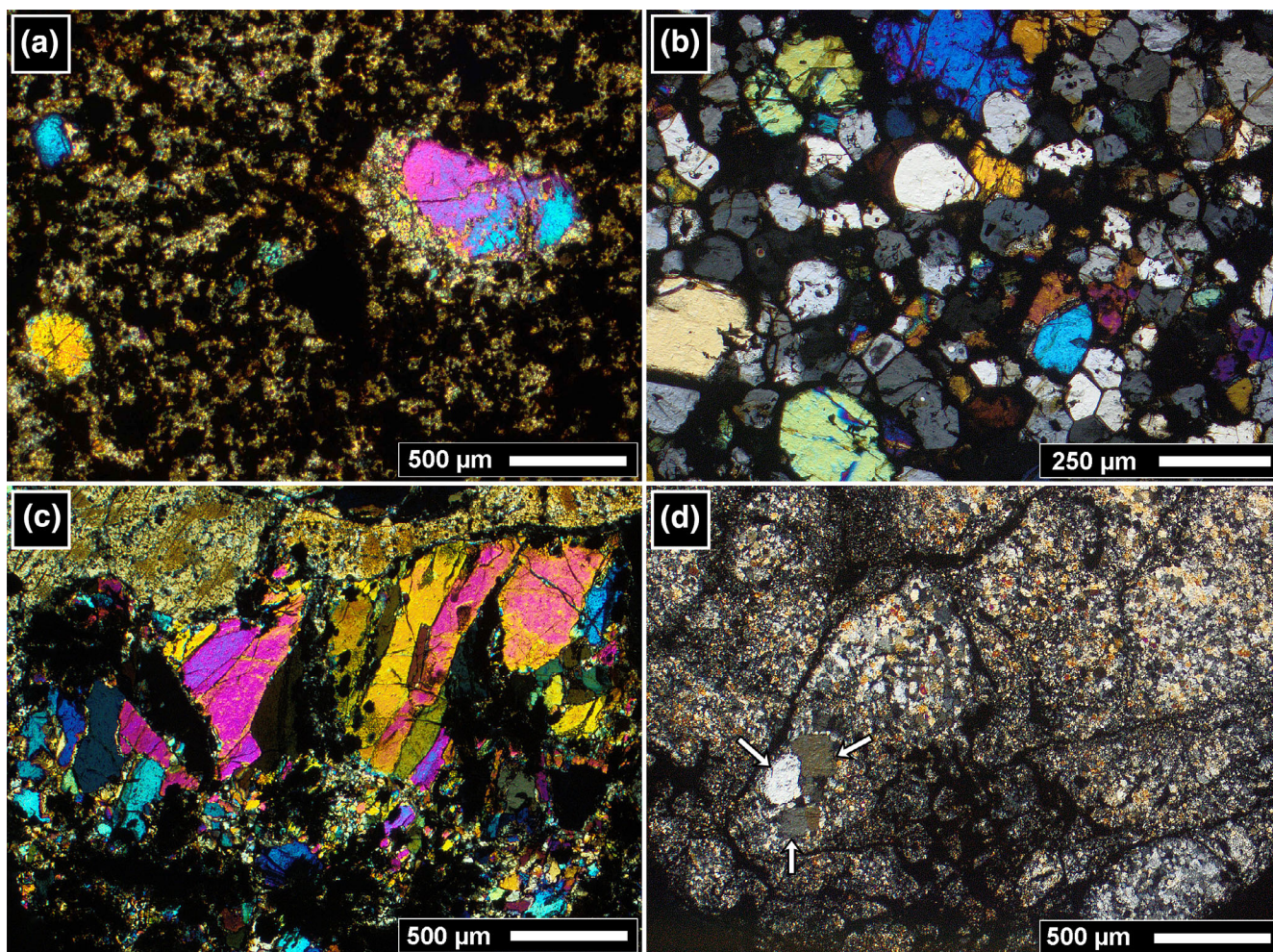


Fig. 8. a) MS-MU-021 is a ureilite having some large olivine inclusions embedded in a typical fine-grained lithology. b) Pyroxene-rich ureilite MS-316 has a medium-sized texture with some large olivines. c) MS-MU-028 has an unusual texture with oriented olivine. d) Most parts of MS-250 are fine grained, but areas with large ($>100\ \mu\text{m}$; arrows) mafic crystals are also present. Images (a–d) in transmitted light, crossed nicols. (Color figure can be viewed at wileyonlinelibrary.com.)

the chondrites are shock-darkened (e.g., MS-151, MS-262), and the H5/6 chondrite MS-11 contains shock-melted areas (Horstmann & Bischoff, 2014).

The Unique R-Like Chondrite

AhS fragment MS-CH (Horstmann, 2010; Horstmann & Bischoff, 2010a, 2014; Horstmann et al., 2010; Riebe et al., 2014, 2017) shows many features that are similar to Rumuruti (R) chondrites (Fig. 17) (Bischoff et al., 2011). As earlier summarized, the olivine-rich rock (Fa_{35-37}) of petrologic type 3.8 ± 0.1 has an oxygen isotope composition close to that of R chondrites, a matrix abundance of $\sim 45\ \text{vol}\%$, and a mean chondrule size of $\sim 450\ \mu\text{m}$ (Horstmann & Bischoff, 2014; Horstmann et al., 2010). However, the metal abundance of some vol% (Fig. 17) or the absence

of magnetite and platin-group element-rich phases such as sulfides, tellurides, and arsenides clearly distinguish the AhS fragment MS-CH from other type 3 R chondrites (Bischoff, 2000; Bischoff et al., 2011).

The Carbonaceous Chondrite (CB_a)

MS-181 is a metal-rich rock ($\sim 60\ \text{vol}\%$ metal; Fig. 18a) and contains silicates of various textures (Bischoff et al., 2012; Horstmann & Bischoff, 2014; Riebe et al., 2017). The overall texture is similar to characteristics described by Krot et al. (2007) and Rubin et al. (2003) for CB_a -chondrites. The rock contains large kamacite globules (up to $\sim 8\ \text{mm}$) with highly variable abundances of Cr-bearing FeS inclusions (Fig. 18b). Thus, the subtexture is similar to those in the CB_a chondrite Gujba (Krot et al., 2007).

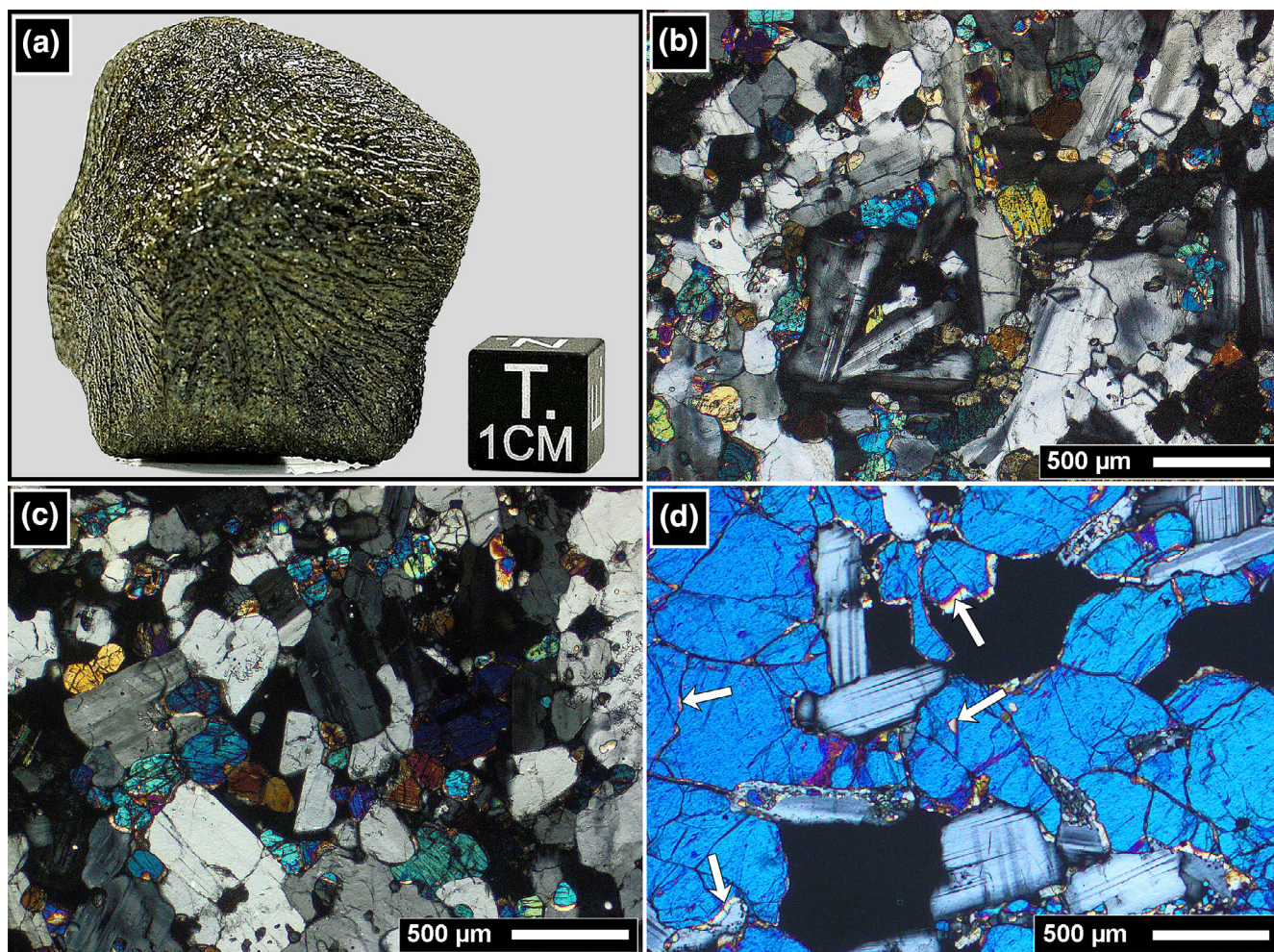


Fig. 9. a) Trachyandesite MS-MU-065 nicely shows flight-oriented features. MS-277 (b) and MS-MU-035 (c) consist of abundant anorthoclase (gray). d) A small part of a centimeter-sized olivine (Fa_{39}) in the trachyandesite MS-MU-011 encloses plagioclase (cores: $\sim\text{An}_{53}$) and small low-Ca pyroxenes (yellowish, arrows). Images (b–d) in transmitted light, crossed nicols. (Color figure can be viewed at wileyonlinelibrary.com.)

DISCUSSION

Abundances of Ureilitic and Non-Ureilitic Rocks

Since the 2014 review concerning the 110 AhS stones studied worldwide (Horstmann & Bischoff, 2014), new data on a distinctly greater number of AhS samples have not significantly changed the numbers of earlier estimates concerning the abundances of ureilitic and non-ureilitic lithologies. Horstmann and Bischoff (2014) reported an abundance of 31.8% chondrites from the studied AhS stones (35 chondrites among 110 registered samples). Within the sample set, 30 chondrites ($\sim 36\%$) were present among the 82 samples examined at the University of Münster (e.g., Bischoff et al., 2012; Bischoff, Horstmann, Laubenstein, et al., 2010; Bischoff, Horstmann, Pack, et al., 2010; Horstmann,

Bischoff, et al., 2012; Horstmann et al., 2010). Kohout et al. (2010) suggested an even higher abundance of non-ureilitic samples and estimated that about 50% of their 60 samples studied could be of non-ureilitic origin. Considering hand specimen properties, Shaddad et al. (2010) estimated $\sim 20\text{--}30\%$ of non-ureilitic samples and found that this percentage was similar among the large ($\sim 100\text{ g}$) as well as among the small ($\sim 1\text{ g}$) fragments of the collected rocks. Considering the 249 samples described in the current study, we classified 81 (33%) non-ureilitic samples and 166 (67%) samples of ureilitic origin. Clearly, as already stated above, the data are very similar to those published about 10 yr ago. The most abundant samples are coarse-grained ureilites followed by the fine-grained ones (Table 1; Fig. 19). The most spectacular samples of ureilitic origin are the four trachyandesites. The most abundant

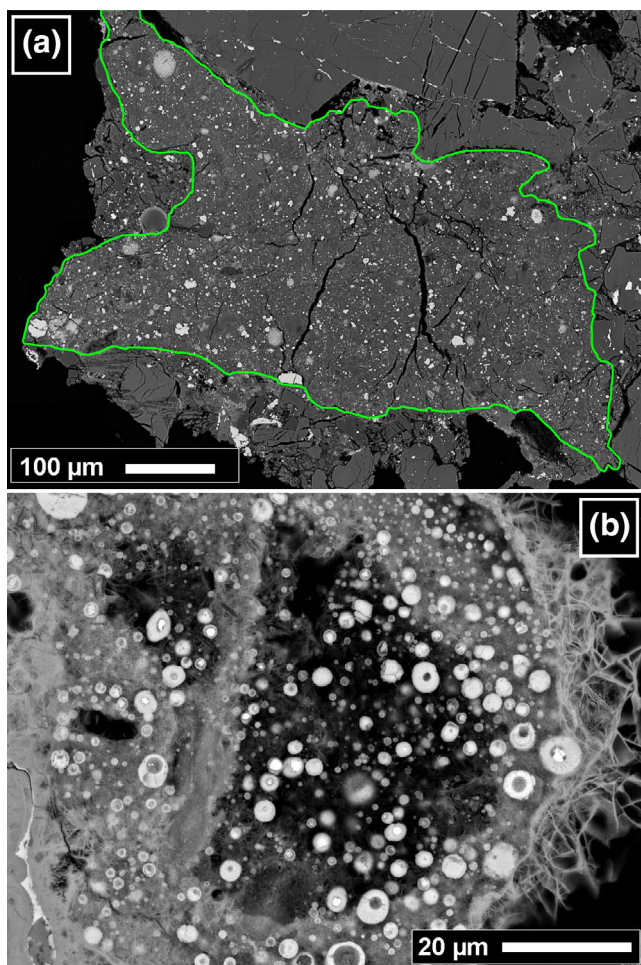


Fig. 10. a) C1 fragment within the ureilitic breccia MS-266. The light particles either represent magnetite or pyrrhotite. b) MS-296 is a fine-grained ureilite breccia containing several areas with unique material containing abundant metal-sulfide-rich spherules. BSE images. (Color figure can be viewed at wileyonlinelibrary.com.)

non-ureilitic samples are E chondrites followed by OC (Fig. 8). The discovery of three samples of a new type of enstatite achondrite is a remarkable result of this survey.

All AhS stones must be regarded as individual specimens that evolved independently from each other after they had been ejected from their original parent bodies and were incorporated into asteroid 2008 TC₃. Thus, the explosion of asteroid 2008 TC₃ in the atmosphere delivered hundreds to thousands of fresh meteorites that had previously been embedded as rocks (perhaps like pebbles) within the fine-grained, carbonaceous host materials of the meteoroid. If the stones were collected hundreds or thousands of years later, most would have been recognized as individual meteorite finds. Only certain types of stones (e.g., the enstatite achondrites, trachyandesites), and ureilites or

enstatites with similar texture and mineralogy would probably be considered paired finds.

What Do the Observed Fragments Tell Us About the Nature of the Accreting Materials or Their Incorporation into Asteroid 2008 TC₃?

As mentioned in the Introduction, without the discovery of non-carbonaceous samples in the AhS strewn field, asteroid 2008 TC₃ would have been considered a C-type (carbonaceous) meteoroid based on spectral observations alone. One can speculate even further: Considering the mass calculations, observations during and after the entry of the atmosphere, the mineralogy of the samples AhS 91A and AhS 671, and experimental work to fit the asteroid spectrum (Goodrich et al., 2019; Shaddad et al., 2010), the overwhelming portion of the meteoroid (~99%, per data of Shaddad et al. [2010] on the size of the asteroid and the density of the meteorite finds) was likely made of the fine-grained dust (carbonaceous, probably C1 material) and was lost in the atmosphere.

Considering the broad spectrum of different chondritic and achondritic meteorite types, some interesting observations can be made:

1. All achondritic fragments indicate processes of reduction: They are either ureilitic in origin and probably experienced a reduction process during destruction of the ureilite parent body (UPB) or are reduced lithologies as presented by the metal-rich E achondrites similar to Itqiy and Northwest Africa 2526 (e.g., Humayun et al., 2009; Keil & Bischoff, 2008; Patzer et al., 2001).
2. One CB chondrite fragment was found in this study. This type of carbonaceous chondrite is a reduced subtype and characterized by a high metal abundance and Fe-poor silicates.
3. Abundant fragments in asteroid 2008 TC₃ represent all kinds of enstatite (E) chondrites, which belong to the most reduced chondrites in general.
4. Considering the 11 studied OCs, it is obvious that except for one L- and one LL-type chondrite, all belong to the H chondrites, the most reduced type of OC.
5. Sample MS-CH is classified as a unique chondrite with affinities to the Rumuruti chondrites, when the Fa and Fs contents of olivine and pyroxene, respectively, are considered indicating formation in more oxidizing conditions. However, MS-CH is very different to the oxidized R chondrites in having some vol% of metal (Horstmann et al., 2010), which is completely absent in R chondrites (Bischoff et al., 2011).

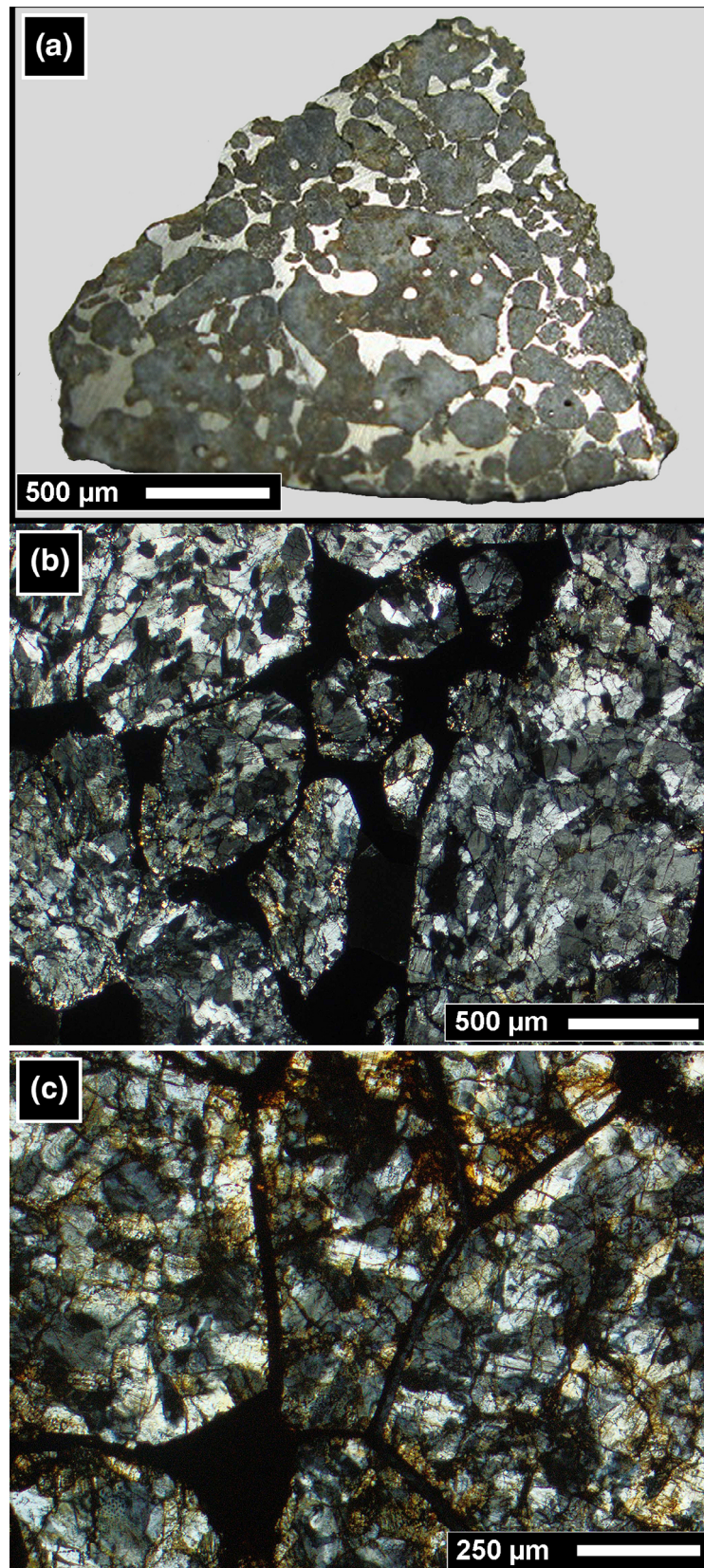


Fig. 11. a) In sample MS-MU-019, the silicates (gray) are enclosed by a network of metals (white); width: ~2.4 cm. b) MS-MU-036 contains pyroxene-rich areas and metals (black). c) Texture of the pyroxene-rich sample MS-245. Images in (b) and (c) in polarized light, crossed nicols. (Color figure can be viewed at wileyonlinelibrary.com.)

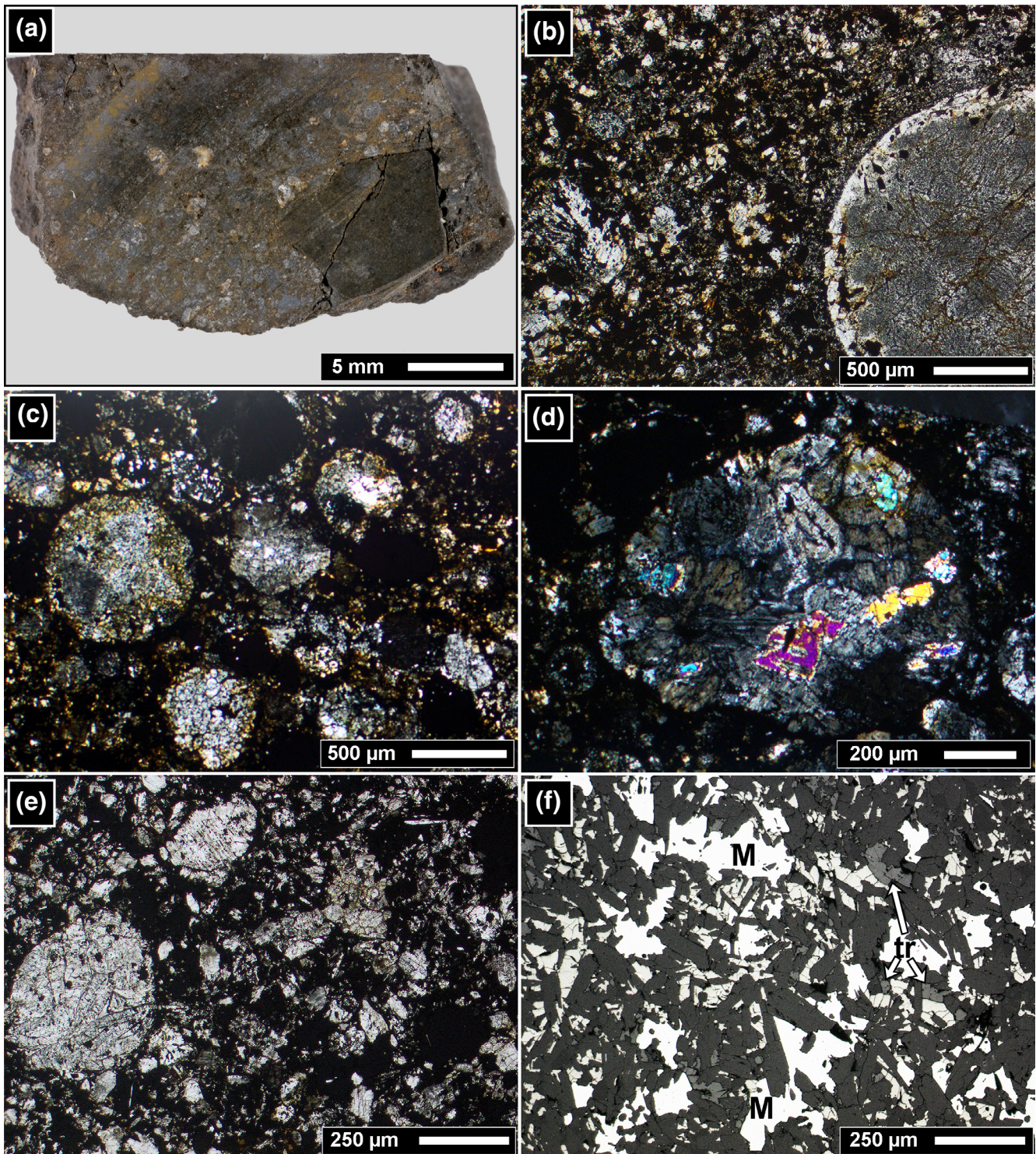


Fig. 12. E chondrites. a) Cut surface of the enstatite chondrite breccia MS-179. b) MS-MU-058 (EL_b5) with a 2 mm-sized recrystallized chondrule. c) MS-MU-031 (EL_a3) with olivine in a (d) porphyritic chondrule. e) MS-300 (EH_a4). f) MS-MU-039 (EL melt breccia) with abundant enstatite laths (black) embedded in metal (M; white) and troilite (tr; light yellowish gray). Images (f) in reflected light, (b–e) in transmitted light. (Color figure can be viewed at wileyonlinelibrary.com.)

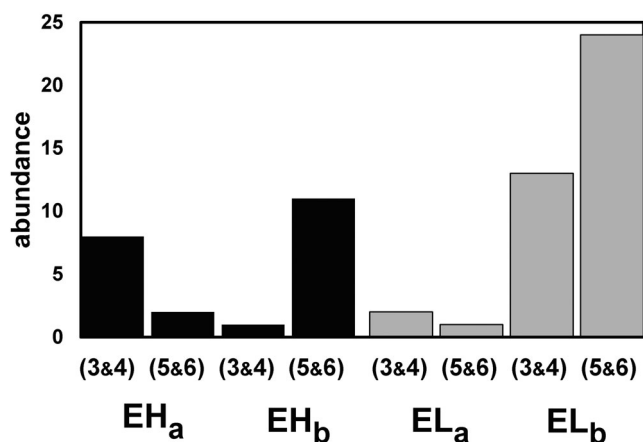


Fig. 13. Abundances of various types of E chondrites from the Almahata Sitta strewn field. EL chondrites are more abundant than EH chondrites. Most abundant are the EL_b5 + EL_b6 chondrites. Not included in the diagram are the E chondrite melt rocks and breccias MS-179 (Fig. 12a), MS-MU-039 (Fig. 12f), and MS-MU-055.

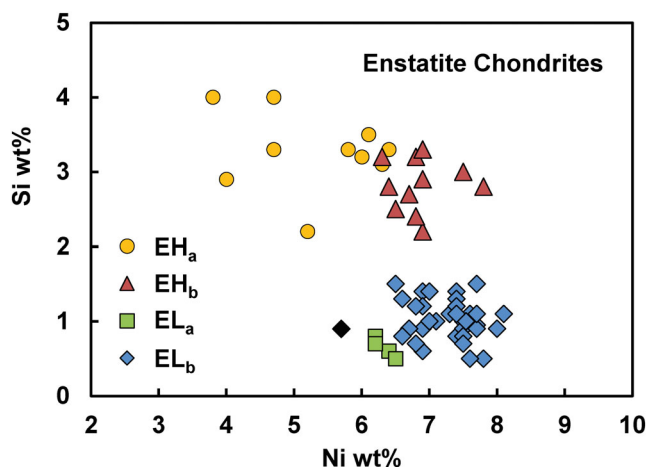


Fig. 14. Mean Ni and Si concentrations in metal from enstatite chondrites. The four groups are well distinguished based on metal compositions and Cr-concentrations in troilite (Weyrauch et al., 2018). The latter is not shown here. The only exception is MS-MU-015 (black diamond) which has unusually low Ni concentrations in metals, but Cr and Fe concentrations in troilite and niningerite/alabandite, respectively, match the characteristics of EL_b chondrites (Weyrauch et al., 2018). (Color figure can be viewed at wileyonlinelibrary.com.)

In summary, all compact fragments from the carbonaceous (C1-dominated) 2008 TC₃ asteroid studied here (1) contain highly reduced components (metals), and (2) most indicate formation in a reducing environment (parent body) over an oxidized one (e.g., E chondrites and E achondrites, CB_a) or (3) have seen a (sudden) reduction event (ureilites). They were all embedded in carbonaceous (C1) host materials. This finding may have consequences considering the orbits of

various types of early formed grand parent (precursor) bodies that delivered fragments by impact during a late accretion of asteroid 2008 TC₃. In this respect, several important questions remain, which we will try to answer below:

1. Were the rocks incorporated during early accretion, or do they represent fragments resulting from late impacts?
2. When did the (possible) early accretion take place, or when were the rocks (xenoliths) incorporated in the early accreted parent body?

It should be mentioned for completeness that one amphibole-bearing stone (AhS 202) was recently described that may be related to a unique type of carbonaceous chondrite (Goodrich et al., 2020; Hamilton et al., 2020). The relationship of this AhS stone to all others is unclear.

What Do the Observed Fragments Tell Us About Early or Late Accretion/Incorporation of/into 2008 TC₃?

Considering the age of accretion/incorporation into the parent body of asteroid 2008 TC₃, Goodrich, Sanborn, et al. (2021) focused on the evolution of the chondrites. They highlighted that Blackburn et al. (2017) could convincingly show, based on Pb-Pb closure ages, that type six OC per se did not exist until 40–60 Ma after calcium–aluminum-rich inclusions (CAIs). Thus, considering the time of accretion/incorporation, metamorphosed OC—and we think metamorphosed enstatite chondrites as well—could not have been available before this time. Goodrich, Sanborn, et al. (2021) also mentioned that for type 4 and 5, less time is required: ~10–40 and ~30–50 Ma, respectively (Blackburn et al., 2017). Keeping these ages in mind, additional time for the transport of materials after the catastrophic impact is required to bring the materials from various depths of the destroyed parent bodies (several different classes of OCs, ECs) to the location of accretion/incorporation.

Another interesting piece of information comes from the brecciated enstatite chondrite MS-179 (Fig. 12a), which is a complicated breccia consisting of type 3 components as well as of type 5 lithologies. Before becoming a part of the asteroid 2008 TC₃ parent body, the tough breccia must have been formed on a chondritic enstatite parent body. This means that on the enstatite parent body, the following steps occurred before ejection from the parent body and accretion/incorporation of/into asteroid 2008 TC₃:

1. accretion of chondritic materials (of course, after chondrule formation),

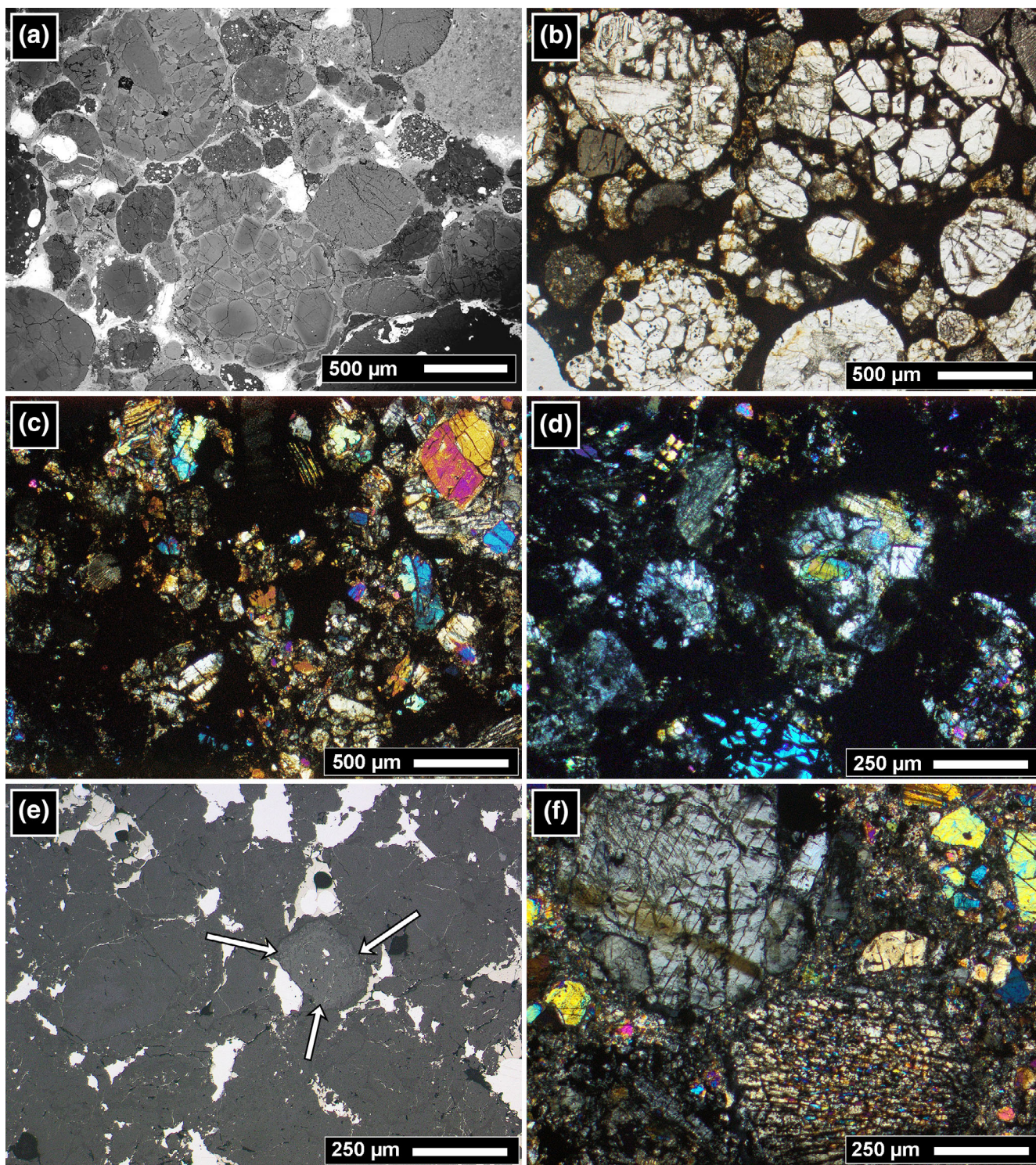


Fig. 15. Ordinary chondrites. a, b) MS-MU-060 is a highly unequilibrated L3 chondrite with well-defined chondrules embedded in an opaque matrix; (a) BSE image and (b) image in plane-polarized transmitted light. c) MS-280 (H4/5). d) MS-MU-043 (H4). e) MS-312 (H5) with a Cr-spinel-rich object in the center, which represents a metamorphosed calcium–aluminum-rich inclusion (arrows; BSE-image). f) LL4 chondrite MS-197. Images (c, d, and f) in transmitted light, crossed nicols. (Color figure can be viewed at wileyonlinelibrary.com.)

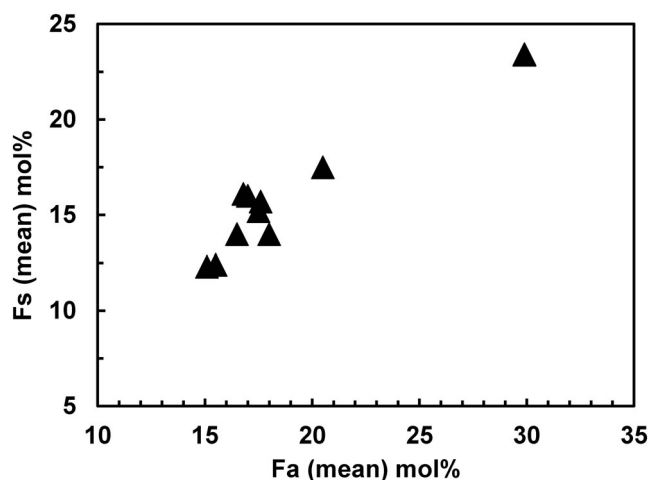


Fig. 16. Mean compositions of olivine and low-Ca pyroxene in the equilibrated ordinary chondrites from the Almahata Sitta strewn field studied in Münster. The L3 chondrite MS-MU-060 is not shown due to the large variations in Fa (14.5 ± 9.9 mol%) and Fs contents (10.5 ± 7.6 mol%).

2. metamorphism to form a type 5 lithology,
3. impact-induced mixing of different lithologies,
4. lithification and breccia formation, and finally,
5. impact destruction and ejection of MS-179-like components.

All these processes certainly must have taken a long time (particularly considering the previously mentioned time span constraints for metamorphosed OCs by Blackburn et al. [2017]) before accretion/incorporation of/into the asteroid 2008 TC₃ parent body could have occurred subsequently.

Previously, studies have suggested that the time span during which asteroid 2008 TC₃ traveled through space after its break-off was on the order of ~20 Ma (Welten et al., 2010). Furthermore, Riebe et al. (2017) showed that the chondritic samples have a somewhat larger variation in cosmic ray exposure (CRE) ages (16–22 Ma) than the ureilitic ones (18–22 Ma; Welten et al., 2010) and that an E chondrite breccia (MS-179) has a CRE age of only ~11 Ma. This is quite surprising, since MS-179 already experienced breccia formation by impact lithification (e.g., after mixing of type 5 and unmetamorphosed, near-surface type 3 materials) in (near-)surface locations of the enstatite parent body. Despite having been on the surface of the E chondrite parent body prior to ejection and incorporation/accretion into/of the 2008 TC₃ parent body, this sample has a significantly shorter CRE age than other E chondrite stones that represent highly metamorphosed type 6 lithologies from greater depth of the parent body. The question is, why does a brecciated sample—probably having seen CRE on the surface of its original

parent body—have a lower CRE age than interior type 6 samples? From the studies of the fine-grained C1-related portion of AhS 91A (Goodrich et al., 2019), the situation is even more complex, since this material has an even lower CRE age (~5–9 Ma) than other previously studied AhS stones (11–22 Ma; Riebe et al., 2017; Welten et al., 2010). Thus, considering the proposed model in this study that the C1 lithology is the host, it might make sense that the host lithology has the lowest CRE age of 5–9 Ma, while all exotic clasts have higher CRE ages. However, the question remains open, why most of the AS ureilites and chondrites have ages that cluster around ~20 Ma and do not scatter randomly; an issue that was also discussed by Riebe et al. (2017).

From the discussion above (e.g., formation time of type 6 lithologies), it is clear that appropriate AhS stones (e.g., EL6 and H5 stones) could not have been incorporated into the 2008 TC₃ body or precursor body (if 2008 TC₃ is only a break-off fragment of a once larger asteroid) earlier than 50–100 Ma after CAIs. Thus, as also discussed by Meier et al. (2012), the different CRE ages (11–23 Ma) may (at least partly) result from irradiation of small objects occurring between the time of ejection from their parent bodies (e.g., ureilite, E chondrite, and OC) and accretion of the 2008 TC₃ body (or precursor) or the incorporation of these fragments into the planetary object by late impacts.

Asteroid 2008 TC₃: Mixing (Accretion, Incorporation) of Chondritic and Achondritic Components

Goodrich et al. (2019) described fragments AhS 91A and AhS 671, which are the first AhS stones to show contacts between ureilitic and chondritic materials. A third sample is the polymict sample MS-266 (Fig. 10a), briefly considered in this study. Goodrich et al. (2019) further stated that “the C1-material consists of fine-grained phyllosilicates (serpentine and saponite) and amorphous material, magnetite, breunnerite, dolomite, fayalitic olivine (F_{O28-42}), an unidentified Ca-rich silicate phase, Fe, Ni sulfides, and minor Ca-phosphate and ilmenite”; most of these phases are typically found in other C1 chondrites (e.g., C1I, Flensburg; e.g., Alfing et al., 2019; Bischoff et al., 2021; Fredriksson & Kerridge, 1988; Morlok et al., 2006). Goodrich et al. (2019) also performed experiments by mixing different meteorite analog visible-to-near-infrared reflectance spectra to fit the F-type spectrum of the asteroid and determined that asteroid 2008 TC₃ may have consisted mainly of ureilitic and AhS 91A-like materials. It is remarkable that these results show that the major portion (40–70%) would be C1 material, followed by ureilitic components and <10% of OC, EC, and other meteorite types. They

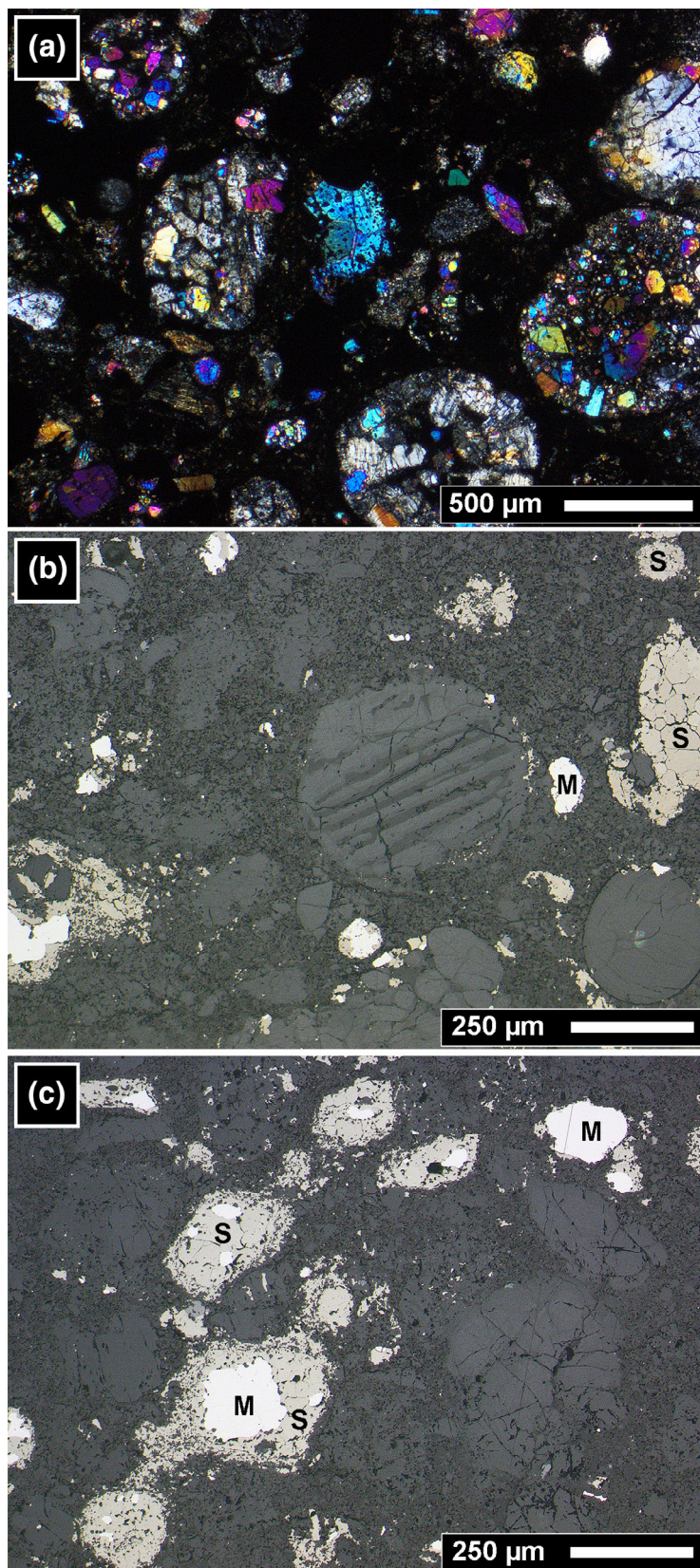


Fig. 17. Representative images of the unique R chondrite-like stone of the AhS strewn field MS-CH having (a, b) a chondritic texture and (c) areas with abundant metals (M, white) often enclosed in sulfides (S, beige). Images (b) and (c) taken in reflected light. (Color figure can be viewed at wileyonlinelibrary.com.)

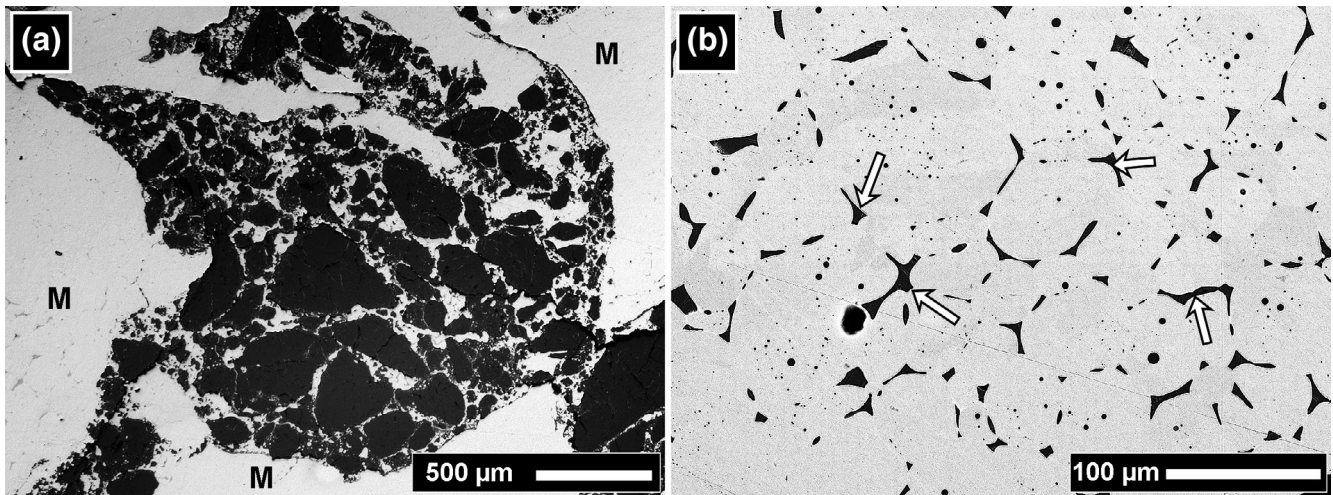


Fig. 18. a) The overall texture of the CB_a individuum MS-181 from Almahata Sitta with abundant metal (M; white) and silicate areas (gray). Image in reflected light. b) BSE image of the internal structure of the metal-rich globules with the sulfide exsolutions (arrows).

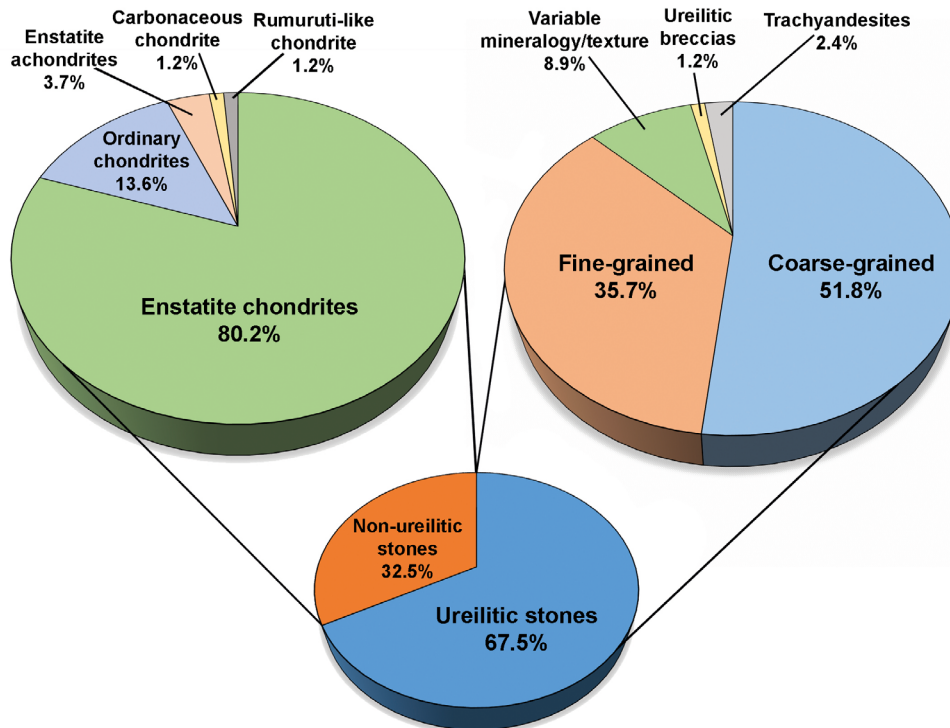


Fig. 19. Distribution of various different rock types from the Almahata Sitta strewn field classified in Münster. A total number of 249 stones were studied. (Color figure can be viewed at wileyonlinelibrary.com.)

further suggested that the bulk density of AhS 91A ($2.35 \pm 0.05 \text{ g cm}^{-3}$) would be close to estimates for the asteroid ($\sim 1.7\text{--}2.2 \text{ g cm}^{-3}$) and that its porosity of 36% would be near the low end of estimates for the asteroid (33–50%), suggesting significant macroporosity. The results of these experiments clearly support earlier

assumptions by Shaddad et al. (2010) that the main portion (particularly considering the volumes of the involved components and their densities) of the exploded meteoroid 2008 TC₃ was of fine-grained materials, as also later supported by Goodrich et al. (2014) that most of this material was probably the

fine-grained matrix material in which the more coherent rock fragments were embedded.

Considering the UPB history, Goodrich, Sanborn, et al. (2021) discussed the possibility that 2008 TC₃ was derived from a volume consisting mainly of carbonaceous chondrite material and that asteroid 2008 TC₃ is from the same regolith from which also the typical polymict ureilites (TPUs) derived—thus, from a ureilitic parent body. This is in contrast to our view. We think that based on all data and observations, there is no indication that the dominating material in asteroid 2008 TC₃ was ureilitic in origin. Instead, the dominating material was carbonaceous. This must lead to the unambiguous consequence that the C1 materials are not xenoliths within ureilitic components; instead, the ureilitic and non-ureilitic rocks are xenoliths in a polymict C1 parent body. We think that this may also explain why the AhS 91A bulk sample does not show a solar wind component (Goodrich et al., 2019) because all components were shielded and instead represent parts of the dominating subsurface layers and/or interior materials. The existence of the AHS 91A and MS-266 breccias containing C1 components can easily be explained by late impact brecciation, mixing, and lithification in the time span between the latest time of accretion and today.

Formation of Asteroid 2008 TC₃ or Its Parent Planetesimal

We will probably never know whether the mineralogy and structure of asteroid 2008 TC₃ body were the same as (or quite similar to) the parent body or whether 2008 TC₃ was only a mineralogically distinct break-off fragment of a once larger asteroid.

We agree with the suggestion of Goodrich et al. (2019) that 2008 TC₃ was a heterogeneous asteroidal breccia, in which the clasts were so loosely bound that they separated in the atmosphere and landed on Earth as individual stones, which would support the view about the pre-impact observations of the ~4 m asteroid 2008 TC₃. However, based on the light curve, the F-type reflectance spectrum (Jenniskens, Shaddad, Numan, et al., 2009; Scheirich et al., 2010), and the proposed 40–70% of C1 matter (Goodrich et al., 2019), a carbonaceous chondrite character has to be strongly considered. Thus, in this study, we suggest that the AhS samples derive from a carbonaceous parent body, a polymict C1 object. The idea that asteroid 2008 TC₃ was not a polymict ureilite is not completely new: Goodrich et al. (2014) mentioned that samples from the AhS strewn field should not even be classified as ureilites but rather as a unique meteoritic breccia.

The formation and evolution of asteroid 2008 TC₃ have been discussed to various extents by several researchers (e.g., Bischoff, Horstmann, Pack, et al., 2010; Goodrich et al., 2014, 2015; Hartmann et al., 2011; Herrin et al., 2010; Horstmann & Bischoff, 2014). In prior discussions, the final catastrophic disruption of the UPB delivering various ureilitic materials in terms of texture and mineral composition has typically been chosen as a starting point for the formation and evolutionary pathway of asteroid 2008 TC₃. But from many observations we have obtained in the meantime, it is clear that the overwhelming material of asteroid 2008 TC₃ was fine-grained, carbonaceous material. Thus, this major component should stay in the focus of all discussions on the formation of the appropriate parent body.

Downes et al. (2008) described different kinds of fragments (including enstatite grains) in polymict ureilites. However, in the past, we also have studied many polymict ureilites in detail, but we never observed typical lithic E chondrite clasts, that is, consisting of more than one enstatite grain or chondrule (Patzek et al., 2018, 2019, 2020, 2021). In our view, the lack of millimeter- to centimeter-sized E chondrite fragments in polymict ureilites—a very abundant type of xenolith in asteroid 2008 TC₃—clearly speaks against a common origin of polymict ureilites and 2008 TC₃-like materials. Thus, we do not agree with the idea that the diversity of non-ureilitic materials in AhS would resemble that material found in TPUs, and that asteroid 2008 TC₃ is a sample of loosely consolidated regolith from the same body as TPUs (Goodrich et al., 2015, 2019; Goodrich, Bottke, et al., 2021; Goodrich, Sanborn, et al., 2021). Goodrich, Bottke, et al. (2021) cited that Bischoff et al. (2006) would have noted that TPUs would contain xenoliths from every major chondrite class (OC, EC, RC, CC) including multiple groups (i.e., H, L, LL, EH, EL) and petrologic types (1–6) of each; this is certainly not correct!

The situation is different when considering only the ureilitic fragments in polymict ureilites. In this respect, Goodrich, Sanborn, et al. (2021) have pointed out that polymict ureilites show the same range of ureilite types as the ureilite collection on the whole (Downes et al., 2008; Goodrich et al., 2004) and that this would indicate that polymict ureilites developed on second-generation offspring bodies rather than on the original UPB. Consequently, we have to follow that all different types of ureilitic lithologies were completely separated from each other—by impact-induced fragmentation—after the disruption of UPB and ejected into space. We will never know how much of this material re-accreted to form the offspring body from which the TPUs derive and how many were formed, but we can consider that

different follow-up parent bodies accreted with different proportions of different ingredients. One of the second-generation parent bodies may be the planetary object from which the TPUs derive, while others may have formed in locations with higher abundances of carbonaceous materials, as found in asteroid 2008 TC₃. In this respect, the C1-dominated asteroid 2008 TC₃ has a much higher abundance of non-ureilitic materials (considering all coarse-grained lithic clasts) compared to <1% in previously studied TPUs (Goodrich et al., 2014).

Horstmann and Bischoff (2014) favored the re-accretion model for the formation of a polymict second-generation asteroid, of which asteroid 2008 TC₃ may represent a certain part, and we will not repeat the early discussion. Herrin et al. (2010) also suggested that the ureilitic fragments formed a debris cloud around the former UPB and were mixed with various chondritic materials, finally forming “polylithologic aggregate objects such as asteroid 2008 TC₃.” In all cases, the abundant fine-grained carbonaceous material has not been considered in these models. That certain breccias contain fragments of various degrees of oxidation has also been noted earlier (e.g., Patzek et al., 2018; Trigo-Rodríguez et al., 2019). In general, meteorites containing foreign clasts are often regolith breccias (e.g., Bischoff et al., 2006; Bischoff, Schleiting, et al. 2018; Bischoff & Stöffler, 1992; Keil, 1982; Stöffler et al., 1988). In the case of rocks from asteroid 2008 TC₃, however, the absence of solar wind gases clearly argues against a regolith nature of asteroid 2008 TC₃ and suggests that the recovered objects were shielded at greater depth in a larger body (e.g., Horstmann & Bischoff, 2014; Meier et al., 2012; Ott et al., 2010; Welten et al., 2010). Until recently, only the compact rocks were analyzed for having solar gases. Since then, it has been found that also the fine-grained AHS 91 stone does not contain solar gases (Goodrich et al., 2019; Goodrich, Sanborn, et al., 2021). Therefore, the lack of solar wind-implanted gases in AHS 91a clearly rules out the possibility that the fine-grained carbonaceous material represents surface regolith. Since the CRE ages are highly variable (~5–22 Ma; e.g., Goodrich et al., 2019; Meier et al., 2012; Riebe et al., 2017; Welten et al., 2010), it has to be concluded that all the samples with the higher CRE age must have had some pre-exposure. This may favor the re-accretion model to form a second-generation parent body, although an incorporation of some projectiles during the travel through space can never be ruled out (e.g., Bischoff et al., 2006; Keil, 1982; Trigo-Rodríguez, 2015). Thus, we follow that the co-accretion of compact non-ureilitic and ureilitic rock fragments (perhaps as

pebbles) and high abundances of fine-grained carbonaceous C1 matter (50–100 Ma after CAIs) are certainly favored for parent body formation over models discussing the incorporation of non-ureilitic fragments by late impacts into the regolith of a second-generation ureilitic parent body. Clearly, the formation by re-accretion requires the early existence of a (perhaps “loosely compacted”) precursor parent body, on which aqueous alteration took place prior to destruction. Subsequently, such a body was transported into (probably) inner solar system regions where it was destroyed and where the produced C1-dust and C1-aggregates re-accreted with noncarbonaceous materials, which originally formed under reducing conditions. However, we cannot completely exclude that the C1-materials entered the inner solar system already as dust or loosely consolidated aggregates. These C1-materials occurring as the dominating constituent of asteroid 2008 TC₃ and those C1 clasts occurring as a component in TPUs appear to be derived from the same original precursor body, as revealed by data obtained by the analyses of different isotopic systems (Goodrich et al., 2019; Patzek et al., 2019, 2021).

CONCLUSIONS

From the AhS strewn field, 249 samples are classified and studied in the current study. Of these, 81 (33%) are non-ureilitic samples and 168 (67%) are samples of ureilitic origin. Among the non-ureilitic samples are a large number of different types of enstatite chondrites, which have not been found as centimeter-sized clasts in typical ureilitic breccias before. All AhS stones must be regarded as individual specimens that originally formed independently from each other after they have been ejected from their original parent bodies and were incorporated into asteroid 2008 TC₃. Thus, due to the AhS event, the number of fresh ureilite and enstatite chondrite falls in our meteorite collections increased—in sudden bursts—by several hundred percent. Based on spectroscopic data and the recent identification of C1 lithologies, it is suggested that asteroid 2008 TC₃ mainly consisted of C1 materials. All fragments studied here are somewhat related to a reducing formation process (e.g., enstatite chondrites and achondrites, H chondrites) or a reducing event in their evolution (ureilitic lithologies). This may indicate that the formation of the meteorite parent body of asteroid 2008 TC₃ occurred after the destruction of a C1-dominated small precursor object that had previously traveled inward from the outer solar system. The resulting dust and a small abundance of lithic pebbles then may have re-accreted together into the

parent body. Now, these pebbles appear to be the—by far—dominating recovered samples of the 2008 TC₃ fall and are classified as the AhS stones. Alternatively, the meteorite parent body of asteroid 2008 TC₃ formed after C1 dust—which formed on a destroyed precursor planetesimal in the outer solar system—entered the inner solar system as dust. Anyway, considering all mineralogical and chemical data as well as the spectroscopic observations, we propose that asteroid 2008 TC₃ was a polymict carbonaceous chondrite breccia, specifically a polymict C1.

Acknowledgments—We thank H. Hain, L. Roggon, L. Hilker, and K. Möhlmann for analytical assistance. We acknowledge the helpful reviews of Mike Zolensky and Kees Welten and thank the Associate Editor Josep Trigo-Rodríguez. We also thank Celeste Brenneka for editorial support and Vincent Haberer for providing Fig. 7a. This work is partly funded by the Deutsche Forschungsgemeinschaft (DFG, German Research Foundation)—Project-ID 263649064 – TRR 170 (subproject B05) as well as by Project-ID 413893359 and Project-ID 463342295 (S.E.). This is TRR 170 Publication No. 155. M.P. is partly funded by a Sofja Kovalevskaja Award of the Alexander von Humboldt Foundation. Open access funding enabled and organized by ProjektDEAL.

Data Availability Statement—Data available on request from the authors.

Editorial Handling—Dr. Josep Trigo-Rodríguez

REFERENCES

- Alfing, J., Patzek, M., and Bischoff, A. 2019. Modal Abundances of Coarse-Grained (>5 μm) Components Within CI-Chondrites and Their Individual Clasts—Mixing of Various Lithologies on the CI Parent Body(ies). *Geochemistry—Chemie Der Erde* 79: 125532.
- Amelin, Y., Koefoed, P., Bischoff, A., Budde, G., Brenneka, G., and Kleine, T. 2015. Pb Isotopic Age of ALM-A—A Feldspar-Rich Volcanic Rock from the Crust of the Ureilite Parent Body. *Meteoritics & Planetary Science* 50: 5344.
- Bannemann, L. 2021. Mineralogical and Chemical Characterization of the Polymict Sample MS-266 from the Almahata Sitta Meteorite Strewn Field. Bachelor thesis, Institut für Planetologie, University of Münster.
- Barnes, J. J., Goodrich, C. A., McCubbin, F. M., Bischoff, A., Decker, S., and Boyce, J. W. 2019. Non-Chondritic Volatile Signatures in a Ureilite Trachyandesite (Abstract #1875). 50th Lunar and Planetary Science Conference. CD-ROM.
- Bast, R., Scherer, E. E., and Bischoff, A. 2017. The ¹⁷⁶Lu-¹⁷⁶Hf Systematics of ALM-A: A Sample of the Recent Almahata Sitta Meteorite Fall. *Geochemical Perspectives Letters* 3: 45–54.
- Bischoff, A. 2000. Mineralogical Characterization of Primitive, Type 3 Lithologies in Rumuruti Chondrites. *Meteoritics & Planetary Science* 35: 699–706.
- Bischoff, A., Alexander, C. M. O'D., Barrat, J.-A., Burkhardt, C., Busemann, H., Degering, D., Di Rocco, T. et al. 2021. The Old, Unique C1 Chondrite Flensburg—Insight into the First Processes of Aqueous Alteration, Brecciation, and the Diversity of Water-Bearing Parent Bodies and Lithologies. *Geochimica et Cosmochimica Acta* 293: 142–86.
- Bischoff, A., Ebert, S., Patzek, M., Horstmann, M., Pack, A., Barrat, J.-A., and Decker, S. 2015. New Individuals from the Almahata Sitta Strewn Field: Old Friends and Brand-New Fellows. *Meteoritics & Planetary Science* 50: 5092.
- Bischoff, A., Ebert, S., Patzek, M., Horstmann, M., Pack, A., and Decker, S. 2016. Almahata Sitta News: Well-Known Varieties and New Species in the Zoo (Abstract #6319). *Meteoritics & Planetary Science* 51: A167.
- Bischoff, A., Goodrich, C. A., and Grund, T. 1999. Shock-Induced Origin of Diamonds in Ureilites (Abstract #1100). 30th Lunar and Planetary Science Conference. CD-ROM.
- Bischoff, A., Horstmann, M., Barrat, J.-A., Chaussidon, M., Pack, A., Herwartz, D., Ward, D., Vollmer, C., and Decker, S. 2014. Trachyandesitic Volcanism in the Early Solar System. *Proceedings of the National Academy of Sciences* 111: 12689–92.
- Bischoff, A., Horstmann, M., Heusser, G., Pack, A., and Albrecht, N. 2012. Almahata Sitta Sample MS-181: The First Carbonaceous Chondrite (CB_a) from Asteroid 2008 TC₃. *Meteoritics and Planetary Science* 47: A71.
- Bischoff, A., Horstmann, M., Laubenstein, M., and Haberer, S. 2010. Asteroid 2008 TC₃—Almahata Sitta: Not Only a Ureilitic Meteorite, But a Breccia Containing Many Different Achondritic and Chondritic Lithologies (Abstract #1763). 41st Lunar and Planetary Science Conference. CD-ROM.
- Bischoff, A., Horstmann, M., Pack, A., Herwartz, D., and Decker, S. 2013. Almahata Sitta Sample MS-MU-011: A Rapidly Crystallized Basalt from the Crust of the Ureilite Parent Body. *Meteoritics & Planetary Science* 48: A60.
- Bischoff, A., Horstmann, M., Pack, A., Laubenstein, M., and Haberer, S. 2010. Asteroid 2008 TC₃—Almahata Sitta: A Spectacular Breccia Containing Many Different Ureilitic and Chondritic Lithologies. *Meteoritics & Planetary Science* 45: 1638–56.
- Bischoff, A., Kraemer, A.-K., Klemm, K. I., and Decker, S. 2018. News from the Almahata Sitta Strewn Field—Seven New Samples: Three Ureilites, Three Enstatite Chondrites, and One Ordinary Chondrite (Abstract #6108). *Meteoritics & Planetary Science* 53: A25.
- Bischoff, A., Lentfort, S., Moehlmann, K., Klemm, K., and Haberer, S. 2019. Mineralogical Characteristics of 20 New Samples from the Almahata Sitta Strewnfield. *Meteoritics & Planetary Science* 54: 6030.
- Bischoff, A., Schleiting, M., Wieler, R., and Patzek, M. 2018. Brecciation Among 2280 Ordinary Chondrites—Constraints on the Evolution of Their Parent Bodies. *Geochimica et Cosmochimica Acta* 238: 516–41.
- Bischoff, A., Scott, E. R. D., Metzler, K., and Goodrich, C. A. 2006. Nature and Origins of Meteoritic Breccias. In *Meteorites and the Early Solar System II*, edited by D. S.

- Lauretta and H. Y. McSween Jr., 679–712. Tucson, Arizona: The University of Arizona Press.
- Bischoff, A., and Stöfler, D. 1992. Shock Metamorphism as a Fundamental Process in the Evolution of Planetary Bodies: Information from Meteorites. *European Journal of Mineralogy* 4: 707–55.
- Bischoff, A., Vogel, N., and Roszjar, J. 2011. The Rumuruti Chondrite Group—Invited Review. *Chemie Der Erde—Geochemistry* 71: 101–34.
- Blackburn, T., Alexander, C. M. O'D., Carlson, R., and Elkins-Tanton, L. T. 2017. The Accretion and Impact History of the Ordinary Chondrite Parent Bodies. *Geochimica et Cosmochimica Acta* 200: 201–17.
- Borovicka, J., and Charvát, Z. 2009. Meteosat Observation of the Atmospheric Entry of 2008 TC₃ Over Sudan and the Associated Dust Cloud. *Astronomy & Astrophysics* 507: 1015–22.
- Chesley, S., Codas, P., and Yeomans, D. 2008. Asteroid 2008 TC₃ Strikes Earth: Predictions and Observations Agree. <https://neo.jpl.nasa.gov/news/2008tc3.html> (NASA/JPL, near Earth Object Program).
- Collinet, M., and Grove, T. L. 2020a. Incremental Melting in the Ureilite Parent Body: Initial Composition, Melting Temperatures, and Melt Compositions. *Meteoritics & Planetary Science* 55: 832–56.
- Collinet, M., and Grove, T. L. 2020b. Widespread Production of Silica- and Alkali-Rich Melts at the Onset of Planetesimal Melting. *Geochimica et Cosmochimica Acta* 277: 334–57.
- DeMeo, F. E., Alexander, C. M. O'D., Walsh, K. J., Chapman, C. R., and Binzel, R. P. 2015. The Compositional Structure of the Asteroid Belt. In *Asteroids IV*, edited by P. Michel, F. E. DeMeo, and W. F. Bottke, 13–42. Tucson, Arizona: The University of Arizona Press.
- DeMeo, F. E., Binzel, R. P., Slivan, S. M., and Bus, S. J. 2009. An Extension of the BUS Asteroid Taxonomy into the Near-Infrared. *Icarus* 202: 160–80.
- Downes, H., Mittlefehldt, D. W., Kita, N. T., and Valley, J. W. 2008. Evidence from Polymict Ureilites for a Disrupted and Re-Accreted Single Ureilite Parent Asteroid Gardened by Several Distinct Impactors. *Geochimica et Cosmochimica Acta* 72: 4825–44.
- El Goresy, A., Boyet, M., and Miyahara, M. 2011. Almahata Sitta MS-17 EL-3 Chondrite Fragment: Contrasting Oldhamite Assemblages in Chondrules and Matrix and Significant Oldhamite REE-Patterns. *Meteoritics & Planetary Science* 46: A63.
- El Goresy, A., Lin, Y., Feng, L., Boyet, M., Hao, J., Zhang, J., and Dubrovinsky, L. 2012. Almahata Sitta EL-3 Chondrites: Sinoite, Graphite, and Oldhamite (CaS) Assemblages C- and N-Isotopic Compositions and REE Patterns. *Meteoritics & Planetary Science* 47: A125.
- El Goresy, A., Lin, Y., Miyahara, M., Gannoun, A., Boyet, M., Ohtani, E., Gillet, P. et al. 2017. Origin of EL3 Chondrites: Evidence for Variable C/O Ratios During Their Course of Formation—A State of the Art Scrutiny. *Meteoritics & Planetary Science* 52: 781–806.
- Endreß, M., Keil, K., Bischoff, A., Spettel, B., Clayton, R. N., and Mayeda, T. K. 1994. Origin of Dark Clasts in the Acfer 059/El Djouf 001 CR2 Chondrite. *Meteoritics* 29: 26–40.
- Fredriksson, K., and Kerridge, J. F. 1988. Carbonates and Sulfates in CI Chondrites: Formation by Aqueous Activity on the Parent Body. *Meteoritics* 23: 35–44.
- Funk, C., Bischoff, A., and Schlueter, J. 2011. Xenoliths in Carbonaceous and Ordinary Chondrites (Abstract #5318). *Meteoritics & Planetary Science* 46: A71.
- Gaffey, M. J., Burbine, T. H., and Binzel, R. P. 1993. Asteroid Spectroscopy: Progress and Perspectives. *Meteoritics* 28: 161–87.
- Goodrich, C. A., Bischoff, A., and O'Brien, D. P. 2014. Asteroid 2008 TC₃ and the Fall of Almahata Sitta, A Unique Meteorite Breccia. *Elements* 10: 31–7.
- Goodrich, C. A., Bottke, W. F., Walsh, K. J., and Daly, R. T. 2021. Almahata Sitta Is No More Exotic Than Any Other Polymict Ureilite (Abstract #1331). 52nd Lunar and Planetary Science Conference. CD-ROM.
- Goodrich, C. A., Ebert, S., Bischoff, A., Treiman, A. H., Pack, A., and Barrat, J.-A. 2016. MS-MU-012: A Primary Plagioclase-Bearing Main GROUP Ureilite from Almahata Sitta, with Implications for the Igneous Evolution of the Ureilite Parent Body (Abstract #6105). *Meteoritics & Planetary Science* 51: A292.
- Goodrich, C. A., Fioretti, A. M., Zolensky, M., Shaddad, M., Ross, D. K., Kohl, I., Young, E. et al. 2018. The Almahata Sitta Polymict Ureilite from the University of Khartoum Collection: Classification, Distribution of Clast Types in the Strewn Field, New Meteorite Types, and Implications for the Structure of Asteroid 2008 TC₃ (Abstract #1321). 49th Lunar and Planetary Science Conference. CD-ROM.
- Goodrich, C. A., Hamilton, V. E., Zolensky, M. E., Kita, N. T., Fioretti, A. M., Kohl, I., Young, E. et al. 2020. A Unique Amphibole and Magnetite-Rich Carbonaceous Chondrite Clast from Almahata Sitta (Abstract #1223). 51st Lunar and Planetary Science Conference. CD-ROM.
- Goodrich, C. A., Hartmann, W. K., O'Brien, D. P., Weidenschilling, S., Wilson, L., Michel, P., Young, E. et al. 2015. Origin and History of Ureilitic Material in the Solar System: The View from Asteroid 2008 TC₃ and the Almahata Sitta Meteorite. *Meteoritics & Planetary Science* 50: 782–809.
- Goodrich, C. A., Sanborn, M. E., Yin, Q.-Z., Kohl, I., Frank, D., Daly, R. T., Walsh, K. J. et al. 2021. Chromium Isotopic Evidence for Mixing of NC and CC Reservoirs in Polymict Ureilites: Implications for Dynamical Models of the Early Solar System. *The Planetary Science Journal* 2: 13.
- Goodrich, C. A., Scott, E. R. D., and Fioretti, A. M. 2004. Ureilitic Breccias: Clues to the Petrologic Structure and Impact Disruption of the Ureilite Parent Asteroid. *Geochemistry* 64: 283–327.
- Goodrich, C. A., Zolensky, M., Fioretti, A. M., Shaddad, M. H., Downes, H., Hiroi, T., Young, E. et al. 2019. The First Samples from Almahata Sitta Showing Contacts Between Ureilitic and Chondritic Lithologies: Implications for the Structure and Composition of Asteroid 2008 TC₃. *Meteoritics & Planetary Science* 54: 2769–813.
- Hamilton, V. E., Goodrich, C. A., Treiman, A., Connolly Jr., H. C., Zolensky, M. E., and Shaddad, M. 2020. Discovery of Abundant Tremolite in a Carbonaceous Chondrite Fragment from the Almahata Sitta Meteorite (Abstract #1122). 51st Lunar and Planetary Science Conference. CD-ROM.
- Harries, D., and Bischoff, A. 2020. Petrological Evidence for the Existence and Disruption of a 500 km-Sized Differentiated Planetesimal of Enstatite-Chondritic Parentage. *Earth Planetary Science Letters* 548: 116506.

- Hartmann, W. K., Goodrich, C. A., O'Brien, D. P., Michel, P., Weidenschilling, S. J., and Sykes, M. V. 2011. Breakup and Reassembly of the Ureilite Parent Body, Formation of 2008 TC₃/Almahata Sitta, and Delivery of Ureilites to Earth (Abstract #1360). 42nd Lunar and Planetary Science Conference. CD-ROM.
- Herrin, J. S., Zolensky, M. E., Ito, M., Jenniskens, P., and Shaddad, M. H. 2009. Fossilized Smelting: Reduction Textures in Almahata Sitta Ureilite (Abstract). *Meteoritics & Planetary Science* 44: A89.
- Herrin, J. S., Zolensky, M. E., Ito, M., Le, L., Mittlefehldt, D. W., Jenniskens, P., Ross, A. J., and Shaddad, M. H. 2010. Thermal and Fragmentation History of Ureilitic Asteroids: Insights from the Almahata Sitta Fall. *Meteoritics & Planetary Science* 45: 1789–803.
- Hilker, L. 2017. Metalle und Sulfide in Enstatit-Chondriten. Bachelor thesis, Institut für Planetologie, Westfälische Wilhelms-Universität Münster.
- Hiroi, T., Jenniskens, P. M., Bishop, J. L., and Shatir, T. 2010. Reflectance Spectroscopy of Almahata Sitta Meteorite Samples from Asteroid 2008 TC₃ (Abstract #1148). 41st Lunar and Planetary Science Conference. CD-ROM.
- Hiroi, T., Jenniskens, P., Bishop, J. L., Shatir, T. S. M., Kudoda, A. M., and Shaddad, M. H. 2010. Bi-Directional Visible-NIR and Biconical FT-IR Reflectance Spectra of Almahata Sitta Meteorite Samples. *Meteoritics & Planetary Science* 45: 1836–45.
- Horstmann, M. 2010. Mineralogy and Chemistry of Selected Components in Meteorites. Master thesis, Institut für Planetologie, Westfälische Wilhelms-Universität Münster.
- Horstmann, M. 2013. The Almahata Sitta Meteorites: Insights into the Nature of Selected Chondritic and Achondritic Lithologies and Possible Genetic Relations. PhD thesis, Institut für Planetologie, Westfälische Wilhelms-Universität Münster, Germany.
- Horstmann, M., and Bischoff, A. 2010a. Characterization of Spectacular Lithologies from the Almahata Sitta Breccia (Abstract #1784). 41st Lunar and Planetary Science Conference. CD-ROM.
- Horstmann, M., and Bischoff, A. 2010b. Formation and Evolution of the Highly Unconsolidated Asteroid 2008 TC₃. *Meteoritics & Planetary Science* 45: A83.
- Horstmann, M., and Bischoff, A. 2014. The Almahata Sitta Polymict Breccia and the Late Accretion of Asteroid 2008 TC₃—Invited Review. *Chemie Der Erde—Geochemistry* 74: 149–84.
- Horstmann, M., Bischoff, A., Pack, A., Albrecht, N., Weyrauch, M., Hain, H., Roggon, L., and Schneider, K. 2012. Mineralogy and Oxygen Isotope Composition of New Samples from the Almahata Sitta Strewn Field. *Meteoritics and Planetary Science* 47: A193.
- Horstmann, M., Bischoff, A., Pack, A., and Laubenstein, M. 2010. Almahata Sitta—Fragment MS-CH: Characterization of a New Chondrite Type. *Meteoritics & Planetary Science* 45: 1657–67.
- Horstmann, M., Humayun, M., and Bischoff, A. 2011a. Siderophile Element Patterns of Sulfide-Metal Assemblages from the Almahata Sitta Polymict Breccias. *Meteoritics & Planetary Science* 46: A101.
- Horstmann, M., Humayun, M., and Bischoff, A. 2011b. Rare Earth Element (REE) Abundances of Sulfides from E Chondrite Lithologies of the Almahata Sitta Polymict Breccia. *Meteoritics & Planetary Science* 46: A102.
- Horstmann, M., Humayun, M., and Bischoff, A. 2014. Clues to the Origin of Metal in Almahata Sitta EL and EH Chondrites and Implications for Primitive E Chondrite Thermal Histories. *Geochimica et Cosmochimica Acta* 140: 720–44.
- Horstmann, M., Humayun, M., Fischer-Gödde, M., Bischoff, A., and Weyrauch, M. 2014. Si-Bearing Metal and Niningerite in Almahata Sitta Fine-Grained Ureilites and Insight into the Diversity of Metal on the Ureilite Parent Body. *Meteoritics & Planetary Science* 49: 1948–77.
- Horstmann, M., Humayun, M., Harries, D., Langenhorst, F., Chabot, N. L., Bischoff, A., and Zolensky, M. E. 2012. Wüstite in the Fusion Crust of the MS-166 Almahata Sitta Metal-Sulfide Assemblage. *Meteoritics and Planetary Science* 47: A194.
- Horstmann, M., Humayun, M., Harries, D., Langenhorst, F., Chabot, N. L., Bischoff, A., and Zolensky, M. E. 2013. Wüstite in the Fusion Crust of Almahata Sitta Sulfide-Metal Assemblage MS-166: Evidence for Oxygen in Metallic Melts. *Meteoritics & Planetary Science* 48: 730–43.
- Humayun, M., Keil, K., and Bischoff, A. 2009. Siderophile Elements in Metal from Northwest Africa 2526, an Enstatite Chondrite Partial Melt Residue (Abstract #1744). 40th Lunar and Planetary Science Conference. CD-ROM.
- Hutchins, K. I., and Agee, C. B. 2012. Microprobe Analyses of Two Almahata Sitta Ureilites (Abstract #2435). 43rd Lunar and Planetary Science Conference. CD-ROM.
- Jenniskens, P., Shaddad, M. H., and The Almahata Sitta Consortium 2009. The Unusually Frail Asteroid 2008 TC₃. *Proceedings of the International Astronomical Union* 5: 227–30.
- Jenniskens, P., Shaddad, M. H., Numan, D., Elsir, S., Kudoda, A. M., Zolensky, M. E., Le, L. et al. 2009. The Impact and Recovery of Asteroid 2008 TC₃. *Nature* 458: 485–8.
- Jenniskens, P., Vaubaillon, J., Binzel, R. P., DeMeo, F. E., Nesvorný, D., Bottke, W. F., Fitzsimmons, A. et al. 2010. Almahata Sitta (=Asteroid 2008 TC₃) and the Search for the Ureilite Parent Body. *Meteoritics & Planetary Science* 45: 1590–617.
- Keil, K. 1982. Composition and Origin of Chondritic Breccias. In *Workshop on Lunar Breccias and Soils and Their Meteoritic Analogs*, edited by G. J. Taylor and L. L. Wilkening, 65–83. LPI Technical Report 82-02. Houston, Texas: Lunar and Planetary Institute.
- Keil, K., and Bischoff, A. 2008. Northwest Africa 2526: A Partial Melt Residue of Enstatite Chondrite Parentage. *Meteoritics & Planetary Science* 43: 1233–40.
- Kimura, M., Weisberg, M. K., Takaki, A., Imae, N., and Yamaguchi, A. 2021. An Almahata Sitta EL3 Fragment: Implications for the Complex Thermal History of Enstatite Chondrites. *Progress in Earth and Planetary Science* 8: 55.
- Kohout, T., Jenniskens, P., Shaddad, M. H., and Haloda, J. 2010. Inhomogeneity of Asteroid 2008 TC₃ (Almahata Sitta Meteorites) Revealed Through Magnetic Susceptibility Measurements. *Meteoritics & Planetary Science* 45: 1778–88.
- Kohout, T., Kiuru, R., Montonen, M., Scheirich, P., Britt, D., Macke, R., and Consolmagno, G. 2011. Internal Structure and Physical Properties of the Asteroid 2008 TC₃ Inferred from a Study of the Almahata Sitta Meteorites. *Icarus* 212: 697–700.
- Kowalski, R. A. 2008. 2008 TC₃. In *MPEC 2008-T50*, edited by G. V. Williams, 1. Cambridge, Massachusetts: Minor Planet Center, Smithsonian Astrophysical Observatory.

- Kozubal, M. J., Gasdia, F. W., Dantowitz, R. F., Scheirich, P., and Harris, A. W. 2011. Photometric Observations of Earth-Impacting Asteroid 2008 TC₃. *Meteoritics & Planetary Science* 46: 534–42.
- Krot, A. N., Ivanova, M. A., and Ulyanov, A. A. 2007. Chondrules in the CB/CH-Like Carbonaceous Chondrite Isheyevo: Evidence for Various Chondrule-Forming Mechanisms and Multiple Chondrule Generations. *Chemie Der Erde—Geochemistry* 67: 283–300.
- Lin, Y., El Goresy, A., Boyet, M., Feng, L., Zhang, J., and Hao, J. 2011. Earliest Solid Condensates Consisting of the Assemblage Oldhamite, Sinoite, Graphite and Excess 36S in Lawrencite from Almahata Sitta MS-17 EL3 Chondrite Fragment, Workshop on Formation of the First Solids in the Solar System. Houston (Abstract #9040).
- McGaha, J. E., Jacques, C., Pimentel, E., Garradd, G. J., Beshore, E. C., Boattini, A., Gibbs, A. R. et al. 2008. 2008 TC₃. In *Minor Planet Electronic Circular 2008-TC50*, edited by G. V. Williams (Issued October 6, 14:59 UT), 1. Cambridge, Massachusetts: Minor Planet Center, Smithsonian Astrophysical Observatory.
- Meier, M. M. M., Welten, K. C., Caffee, M. W., Friedrich, J. M., Jenniskens, P., Nishiizumi, K., Shaddad, M. H., and Wieler, R. 2012. A Noble Gas and Cosmogenic Radionuclide Analysis of Two Ordinary Chondrites from Almahata Sitta. *Meteoritics & Planetary Science* 47: 1075–86.
- Meier, M. M. M., Welten, K. C., Jenniskens, P., Baur, H., and Wieler, R. 2010. Cosmic Ray Exposure Ages for Almahata Sitta Non-Ureilite Samples. *Meteoritics & Planetary Science* 45: A135.
- Mikouchi, T., Zolensky, M. E., Ohnishi, I., Suzuki, T., Takeda, H., Jenniskens, P., and Shaddad, M. H. 2010. Electron Microscopy of Pyroxene in the Almahata Sitta Ureilite. *Meteoritics & Planetary Science* 45: 1812–20.
- Mikouchi, T., Zolensky, M., Takeda, H., Hagiya, K., Ohsumi, K., Satake, W., Kurihara, T., Jenniskens, P., and Shaddad, M. H. 2010. Mineralogy of Pyroxene and Olivine in the Almahata Sitta Ureilite (Abstract #2344). 41st Lunar and Planetary Science Conference. CD-ROM.
- Mittlefehldt, D. W., McCoy, T. J., Goodrich, C. A., and Kracher, A. 1998. Non-Chondritic Meteorites from Asteroidal Bodies. In *Planetary Materials—Reviews in Mineralogy*, vol. 26, edited by J. J. Papike, 4-01–4-170. Washington, D.C.: Mineralogical Society of America.
- Moehlmann, K. 2020. Mineralogische und chemische Charakterisierung neuer Proben aus dem Almahata Sitta Streufeld. Bachelor thesis, Institut für Planetologie, Westfälische Wilhelms-Universität Münster.
- Morlok, A., Bischoff, A., Stephan, T., Floss, C., Zinner, E. K., and Jessberger, E. K. 2006. Brecciation and Chemical Heterogeneities of CI Chondrites. *Geochimica et Cosmochimica Acta* 70: 5371–94.
- Ott, U., Herrmann, S., Jenniskens, P. M., and Shaddad, M. 2010. A Noble Gas Study of Two Stones from the Almahata Sitta Meteorite (Abstract #1195). 41st Lunar and Planetary Science Conference. CD-ROM.
- Patzek, M., Bischoff, A., Ludwig, T., Whitehouse, M., Trieloff, M., Visser, R., and John, T. 2021. O-Isotope Signatures of Olivine and Pyroxene Grains in C1 and CM-Like Clasts. *Meteoritics & Planetary Science* 56: 6096.
- Patzek, M., Bischoff, A., Visser, R., and John, T. 2018. Mineralogy of Volatile-Rich Clasts in Brecciated Meteorites. *Meteoritics & Planetary Science* 53: 2519–40.
- Patzek, M., Hoppe, P., Bischoff, A., Visser, R., and John, T. 2020. Hydrogen Isotopic Composition of CI- and CM-Like Clasts from Meteorite Breccias—Sampling Unknown Sources of Carbonaceous Chondrite Material. *Geochimica et Cosmochimica Acta* 272: 177–97.
- Patzek, M., Kadlag, Y., Bischoff, A., Visser, R., Becker, H., and John, T. 2019. Chromium Isotopes and Trace Element Concentration of Xenolithic C1 Clasts in Brecciated Chondrites and Achondrites. *Meteoritics & Planetary Science* 54: 6027.
- Patzer, A., Hill, D. H., and Boynton, W. V. 2001. Itqiy: A Metal-Rich Enstatite Meteorite with Achondritic Texture. *Meteoritics & Planetary Science* 36: 1495–505.
- Peterson, L. D., Newcombe, M. E., Nielsen, S. G., Alexander, C. M. O'D., Wang, J., Sarafian, A. R., and Bischoff, A. 2022. The H₂O Content of the ALM-A Ureilitic Trachyandesite (Abstract #1384). 53rd Lunar and Planetary Science Conference. CD-ROM.
- Riebe, M., Welten, K. C., Meier, M. M. M., Caffee, M. W., Nishiizumi, K., Bischoff, A., and Wieler, R. 2014. Cosmic Ray Exposure Ages of Six Chondritic Almahata Sitta Fragments (Abstract 5359). *Meteoritics & Planetary Science* 49: A341.
- Riebe, M. E. I., Welten, K. C., Meier, M. M. M., Wieler, R., Barth, M. I. F., Ward, D., Laubenstein, M. et al. 2017. Cosmic-Ray Exposure Ages of Six Chondritic Almahata Sitta fragments. *Meteoritics & Planetary Science* 52: 2353–74.
- Ross, A. J., Herrin, J. S., Mittlefehldt, D. W., Downes, H., Smith, C. L., Lee, M. R., Jones, A. P., Jenniskens, P., and Shaddad, M. H. 2011. Petrography and Geochemistry of Metals in Almahata Sitta Ureilites (Abstract #2720). 42nd Lunar and Planetary Science Conference. CD-ROM.
- Ross, A. J., Hezel, D. C., Howard, L. E., Smith, C. L., Downes, H., Herrin, J. S., Jenniskens, P., and Shaddad, M. 2011. Petrography and Modal Abundance of Metal in Ureilites: A Combined 2D and 3D Study. *Meteoritics & Planetary Science* 46: A199.
- Rubin, A. E., Kallemeyn, G. W., Wasson, J. T., Clayton, R. N., Mayeda, T. K., Grady, M., Verchovsky, A. B., Eugster, O., and Lorenzetti, S. 2003. Formation of Metal and Silicate globules in Gubba: A New Bencubbin-Like Meteorite Fall. *Geochimica et Cosmochimica Acta* 67: 3283–98.
- Rumble, D., Zolensky, M. E., Friedrich, J. M., Jenniskens, P., and Shaddad, M. H. 2010. Oxygen Isotope Composition of Almahata Sitta (Abstract #1245). 41st Lunar and Planetary Science Conference. CD-ROM.
- Scheirich, P., Durech, J., Pravec, P., Kozubal, M., Dantowitz, R., Kaasalainen, M., Betzler, A. S. et al. 2010. The Shape and Rotation of Asteroid 2008 TC₃. *Meteoritics & Planetary Science* 45: 1804–11.
- Shaddad, M. H., Jenniskens, P., Numan, D., Kudoda, A. M., Elsir, S., Riyadh, I. F., Ali, A. E. et al. 2010. The Recovery of Asteroid 2008 TC₃. *Meteoritics & Planetary Science* 45: 1557–89.
- Stöffler, D., Bischoff, A., Buchwald, V., and Rubin, A. E. 1988. Shock Effects in Meteorites. In *Meteorites and the Early Solar System*, edited by J. F. Kerridge and M. S. Matthews, 202–465. Tucson, Arizona: The University of Arizona Press.
- Storz, J., Ludwig, T., Bischoff, A., Schwarz, W. H., and Trieloff, M. 2021. Graphite in Ureilites, Enstatite Chondrites, and Unique Clasts in Ordinary Chondrites—Insights from the Carbon-Isotope Composition. *Geochimica et Cosmochimica Acta* 307: 86–104.

- Swinbank, R., and O'Neill, A. A. 1994. Stratosphere-Troposphere Data Assimilation System. *Monthly Weather Review* 122: 686–702. http://badc.nerc.ac.uk/view/badc.nerc.ac.uk_ATOM_dataent_ASSIM.
- Tanbakouei, S., Trigo-Rodríguez, J. M., Blum, J., Williams, I., and Llorca, J. 2020. Comparing the Reflectivity of Ungrouped Carbonaceous Chondrites with That of Short Period Comets like 2P/Encke. *Astronomy & Astrophysics* 641: 1–7.
- Tholen, D. J., and Barucci, M. 1989. Asteroid Taxonomy. In *Asteroids II*, edited by R. Binzel, T. Gehrels, and M. Matthews, 298–315. Tucson, Arizona: The University of Arizona Press.
- Trigo-Rodríguez, J. M. 2015. Aqueous Alteration in Chondritic Asteroids and Comets from the Study of Carbonaceous Chondrites. In *Planetary Mineralogy*, vol. 15, edited by M. R. Lee and H. Leroux, 67–87. Chantilly, Virginia: Mineralogical Society of America.
- Trigo-Rodríguez, J. M., Rimola, A., Tanbakouei, S., Cabedo-Soto, V., and Lee, M. R. 2019. Accretion of Water in Carbonaceous Chondrites: Current Evidence and Implications for the Delivery of Water to Early Earth. *Space Science Reviews* 215: 27.
- Visser, R., John, T., Menneken, M., Patzek, M., and Bischoff, A. 2018. Temperature Constraints by Raman Spectroscopy of Organic Matter in Volatile-Rich Clasts and Carbonaceous Chondrites. *Geochimica et Cosmochimica Acta* 241: 38–55.
- Visser, R., John, T., Patzek, M., Bischoff, A., and Whitehouse, M. J. 2019. Sulfur Isotope Study of Sulfides in CI, CM, C2_{ung} Chondrites and Volatile-Rich Clasts—Evidence for Different Generations and Reservoirs of Sulfide Formation. *Geochimica et Cosmochimica Acta* 261: 210–23.
- Ward, D., Bischoff, A., Roszjar, J., Berndt, J., and Whitehouse, M. J. 2017. Trace Element Inventory of Meteoritic Ca-Phosphates. *American Mineralogist* 102: 1856–80.
- Warren, P. H., and Rubin, A. E. 2010. Pyroxene-Selective Impact Smelting in Ureilites. *Geochimica et Cosmochimica Acta* 74: 5109–33.
- Welten, K. C., Meier, M. M. M., Caffee, M. W., Nishiizumi, K., Wieler, R., Jenniskens, P., and Shaddad, M. H. 2010. Cosmogenic Nuclides in Almahata Sitta Ureilites: Cosmic-Ray Exposure Age, Preatmospheric Mass, and Bulk Density of Asteroid 2008 TC₃. *Meteoritics & Planetary Science* 45: 1728–42.
- Weyrauch, M., Horstmann, M., and Bischoff, A. 2014. Chemistry of Sulfides and Metal in Enstatite Chondrites—How Many Parent Lithologies (Bodies)? (Abstract #5280). *Meteoritics & Planetary Science* 49: A433.
- Weyrauch, M., Horstmann, M., and Bischoff, A. 2018. Chemical Variations of Sulfides and Metal in Enstatite Chondrites—Introduction of a New Classification Scheme. *Meteoritics & Planetary Science* 53: 394–415.
- Wlotzka, F. 1993. A Weathering Scale for the Ordinary Chondrites. *Meteoritics* 28: 460.
- Yeomans, D. 2008. NASA/JPL Near-Earth Object Program Office Statement. <http://neo.jpl.nasa.gov/news/2008tc3.html> (4 November 2008).
- Zolensky, M. E., Herrin, J. S., Jenniskens, P., Friedrich, J. M., Rumble, D., Steele, A., Sandford, S. A. et al. 2009. Mineralogy of the Almahata Sitta Ureilite (Abstract). *Meteoritics & Planetary Science* 44: A227.
- Zolensky, M., Herrin, J., Mikouchi, T., Ohsumi, K., Friedrich, J., Steele, A., Rumble, D. et al. 2010. Mineralogy and Petrography of the Almahata Sitta Ureilite. *Meteoritics & Planetary Science* 45: 1618–37.
- Zolensky, M. E., Herrin, J., Mikouchi, T., Satake, W., Kurihara, T., Sandford, S. A., Milam, S. N. et al. 2010. Olivine in Almahata Sitta—Curiouser and Curiouser (Abstract #2306). 41st Lunar and Planetary Science Conference. CD-ROM.

SUPPORTING INFORMATION

Additional supporting information may be found in the online version of this article.

Supplement S1. List of samples from the Almahata Sitta strewn field classified in Münster with their masses and mineralogical details (texture, important mineral compositions).